



The CO₂ system in the Mediterranean Sea: a basin wide perspective

M. Álvarez¹, H. Sanleón-Bartolomé¹, T. Tanhua², L. Mintrop³, A. Luchetta⁴, C. Cantoni⁴, K. Schroeder⁵, and G. Civitarese⁶

¹IEO – Instituto Español de Oceanografía, Apd. 130, A Coruña, 15001, Spain

²GEOMAR Helmholtz Centre for Ocean Research Kiel, Düsternbrooker Weg 20, 24105 Kiel, Germany

³MARIANDA, Tulpenweg 28, 24145 Kiel, Germany

⁴CNR ISMAR – Consiglio Nazionale delle Ricerche, Istituto di Scienze Marine, viale R. Gessi 2, 34123, Trieste, Italy

⁵CNR ISMAR – Arsenal, Tesa 104, Castello 2737/F, 30122 Venice, Italy

⁶OGS – Istituto Nazionale di Oceanografia e di Geofisica Sperimentale, Borgo Grotta Gigante 42/c, 34018 Sgonico, Trieste, Italy

Correspondence to: M. Álvarez (marta.alvarez@co.ieo.es)

Received: 31 July 2013 – Published in Ocean Sci. Discuss.: 29 August 2013

Revised: 30 November 2013 – Accepted: 28 December 2013 – Published: 14 February 2014

Abstract. The Mediterranean Sea (MedSea) is considered a “laboratory basin” being an ocean in miniature, suffering dramatic changes in its oceanographic and biogeochemical conditions derived from natural and anthropogenic forces. Moreover, the MedSea is prone to absorb and store anthropogenic carbon due to the particular CO₂ chemistry and the active overturning circulation. Despite this, water column CO₂ measurements covering the whole basin are scarce. This work aims to be a base-line for future studies about the CO₂ system space-time variability in the MedSea combining historic and modern CO₂ cruises in the whole area. Here we provide an extensive vertical and longitudinal description of the CO₂ system variables (total alkalinity – TA, dissolved inorganic carbon – DIC and pH) along an East-West transect and across the Sardinia-Sicily passage in the MedSea from two oceanographic cruises conducted in 2011 measuring CO₂ variables in a coordinated fashion, the RV Meteor M84/3 and the RV Urania EuroFleets 11, respectively. In this sense, we provide full-depth and length CO₂ distributions across the MedSea, and property-property plots showing in each sub-basin post-Eastern Mediterranean Transient (EMT) situation with regard to TA, DIC and pH.

The over-determined CO₂ system in 2011 allowed performing the first internal consistency analysis for the particularly warm, high salinity and alkalinity MedSea waters. The CO₂ constants by Mehrbach et al. (1973) refitted by Dickson and Millero (1987) are recommended. The sensitivity of the CO₂ system to the atmospheric CO₂ increase, DIC and/or TA changes is evaluated by means of the Revelle and buffer factors.

1 Introduction

The Mediterranean Sea (MedSea hereafter) is a particular system with respect to its physical and biogeochemical oceanography (e.g. Tanhua et al., 2013a). The MedSea is a land-locked sea exporting warm and salty intermediate water into the Atlantic Ocean through the shallow and narrow Strait of Gibraltar affecting the global thermohaline circulation (e.g. McCartney and Mauritzen, 2001). Apart from the shallow open thermohaline cell encompassing the whole Mediterranean basin, two closed deep overturning cells are active in the western and eastern basins, respectively. Additionally, a complex upper layer circulation is present including significant permanent and quasi-permanent eddies.

One of the most relevant biogeochemical characteristics of the MedSea, especially the eastern basin, is the anomalous high Nitrogen to Phosphorous ratio (e.g. Ribera d’Alcalà et al., 2003; Krom et al., 2005; Pujo-Pay et al., 2011). This fact along with the oligotrophic gradient from west to east could be attributed to the difference in the allochthonous nutrient sources in terms of quantity and quality (Ribera d’Alcalà et al., 2003; Ludwig et al., 2010; Schroeder et al., 2010; Krom et al., 2010) and also to the specific hydrodynamic features of the MedSea (Robinson et al., 2001; Millot and Taupier-Letage, 2005; Huertas et al., 2012).

With a limited exchange with the ocean and its specific circulation, the MedSea is considered a “laboratory basin” (e.g. Robinson and Golnaraghi, 1994; Bergamasco and Malanotte-Rizoli, 2010) where processes occurring on a global scale can be approximated to smaller time and space

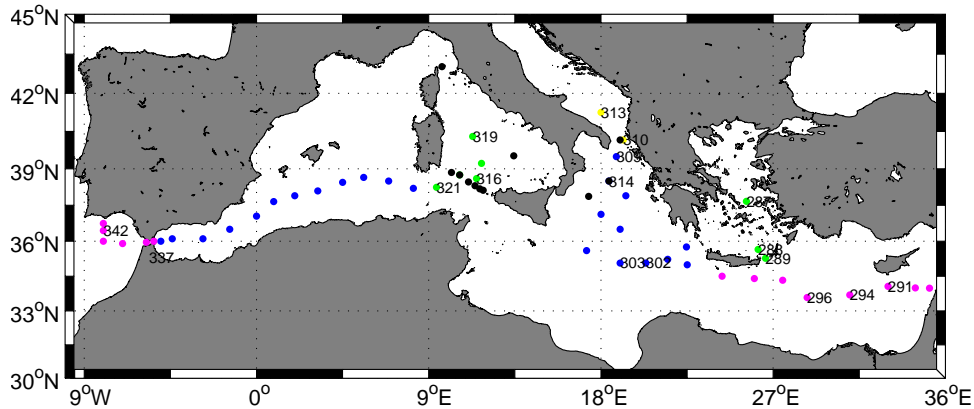


Fig. 1. Map of the Mediterranean Sea with the stations from the Meteor M84/3 (colour dots) and Urania EF11 (black dots) cruises where CO₂ measurements were taken. The colour code for the M84/3 stations corresponds to the data showed in Figs. 12–14.

scales. This fact mostly mentioned for general circulation studies can also be applied for biogeochemical studies, eutrophication, hypoxia, acidification, etc.

The MedSea represents only 0.8 % of the global oceanic surface and despite the general sparseness of water column CO₂ measurements (Álvarez, 2012) it has been identified as an important anthropogenic carbon storage where the column inventory is much higher than in the Atlantic or Pacific oceans (Schneider et al., 2010; Lee et al., 2011). The reasons for this are the intrinsic physico-chemical characteristics of the MedSea where warm and high alkalinity waters, thus low Revelle factor, are prone to absorb CO₂ from the atmosphere and be transported to the interior by the active overturning circulation. With regard to interior CO₂ data, the published literature discussed specific cruises, in the eastern MedSea sub-basins (e.g. Schneider et al., 2010; Luchetta et al., 2010; Krasakopoulou et al., 2011) and the western MedSea (e.g. Brunet et al., 1984; Claustre et al., 2001; Copin-Montegut, 1993; Millero et al., 1979). Cruises covering the eastern and western MedSea are few: the TRANSMED cruise in 2007 (Rivaro et al., 2010), BOUM in 2008 (Touratier and Goyet, 2012), ours in 2011 and the not yet published MedSeA 2013 cruise (medseaoceanruise.wordpress.com).

This paper is a contribution to the Special Issue “Physical, chemical and biological oceanography of the Mediterranean Sea”. In particular, it focuses on CO₂ system analysis performed on board RV Meteor (M84/3 cruise) and RV Urania (EuroFleets 11 cruise), both sampled the MedSea in April 2011 (Tanhua et al., 2013a) (Fig. 1). Besides characterising the particular chemistry of the CO₂ in the MedSea, we will present and discuss vertical distributions and property-property plots in order to present a quasi-synoptic picture of the post-EMT oceanographic situation with regard to the CO₂ system. For those not familiar, briefly, the EMT was a dramatic event changing the hydrography and the large-scale circulation of deep waters in the eastern MedSea, which

changed the formation area from the Adriatic to the Aegean Sea in the 1990s (e.g. Roether et al., 1996, 2007).

2 Data and methods

2.1 Meteor M84/3 cruise

During the Meteor M84/3 cruise in April 2011 (Fig. 1) (Tanhua et al., 2013a, b) Dissolved Inorganic Carbon (DIC), pH and Total Alkalinity (TA) were measured in all stations and depths in order to have an over-determined CO₂ system. Details about the sampling, analysis and quality control are given in Tanhua et al. (2013b). The bottle data is available at the Carbon Dioxide Information Analysis Center (CDIAC) (Tanhua et al., 2012).

The DIC content was determined using a SOMMA instrument. Samples were collected in borosilicate bottles according to standard operation protocol. The precision of the analysis was determined to $\pm 0.6 \mu\text{mol kg}^{-1}$ by titration of several bottles filled from the same Niskin bottle. The accuracy was determined to be $2.5 \mu\text{mol kg}^{-1}$ by analysing a total of 42 bottles of certified reference material (CRM, Andrew Dickson, Scripps, CA, USA, batch 108); the DIC of this batch is certified at $2022.70 \pm 0.7 \mu\text{mol kg}^{-1}$. Measurements of the CRMs were also used to daily correct the temporal drift in the coulometer cell; this correction was never larger than $3 \mu\text{mol kg}^{-1}$.

pH was measured in cylindrical optical glass 10-cm path-length cells with a spectrophotometric procedure (Clayton and Byrne, 1993). pH is reported in the total scale at 25 °C (pH_{25T}). The precision was estimated to ± 0.0012 by measuring replicates from the same Niskin bottle. Regarding the accuracy, the theoretical pH_{25T} value for the 108 CRM batch using the dissociation constants from Mehrbach et al. (1973) refitted by Dickson and Millero (1987) is 7.8782. Replicate pH measurements along the cruise on CRMs are lower than

the theoretical value by 0.0962 ± 0.0012 pH units. We will discuss this point in Sect. 3.2.

Samples for TA determination were collected in 600 mL borosilicate bottles and were analysed within one day after sampling. The TA samples were analysed following the double end point potentiometric technique by Pérez and Fraga (1987) and Pérez et al. (2000). Measurements of CRM were performed in order to control the accuracy of the TA measurements; the pH as measured by the electrode was corrected to obtain the closest mean TA to the CRM; the pH correction was never larger than 0.05. The precision of the TA measurements was better than $0.6 \mu\text{mol kg}^{-1}$ determined from duplicate Niskin bottles, and the accuracy of the TA measurements (i.e. including sampling errors) is determined to be $1 \mu\text{mol kg}^{-1}$. Additionally, the daily drift of the system was determined by regular measurements of a substandard (surface seawater); this drift was always very low.

Other data used in this study from the M84/3 cruise are the hydrographic variables from CTD (Conductivity Temperature Depth) casts, and the bottle data for dissolved oxygen measured by a Winkler potentiometric technique and inorganic nutrients measured with a Quattro auto-analyser. See Tanhua et al. (2013b) for more details. The Apparent Oxygen Utilisation (AOU) is calculated using the saturation equation from Benson and Krause (1984).

2.2 Urania EF11 cruise

During the EF11 survey, samples for DIC, pH and TA were collected and measured on land. Unfortunately, fewer stations (15 for TA and pH, and 9 for DIC) than originally planned (Tanhua et al., 2013b) were sampled due to the geopolitical situation in the area. Two inter-calibration stations with the M84/3 cruise in the Ionian Sea were occupied (Fig. 1). All samples were carefully sampled in borosilicate glass bottles, poisoned with mercuric chloride, sealed with grease (silicone) and stored in the dark at a constant temperature of about 12 °C, until the analyses in the laboratories on shore (ISMAR for TA and pH and GEOMAR for DIC).

In ISMAR pH was measured as described in the previous section, with the spectrophotometric procedure described by Clayton and Byrne (1993), and reported at 25 °C and on the Total scale. The precision was estimated to be ± 0.003 measuring replicates from the same Niskin bottle. Regarding the accuracy, the theoretical pH_{25T} value for the CRM batch 100, using the dissociation constant from Mehrbach et al. (1973) refitted by Dickson and Millero (1987), is 7.907. Our pH replicates on CRMs batch 100 are lower than the theoretical value by 0.019 ± 0.003 pH units. We further checked the accuracy against Tris Buffer Solution Synthetic Seawater batch 13 (distributed by Dr. Dickson), with certified pH corresponding to 8.093 pH_{25T}. Our replicates on Tris are lower than the theoretical value by 0.018 ± 0.004 . As the two different accuracies match very well, this correction was applied to the EF11 pH values.

TA was determined by potentiometric titration in an open cell with a difference derivative readout (Hernandez-Ayon et al., 1999). The precision of the TA measurements was better than $2.3 \mu\text{mol kg}^{-1}$ determined from duplicate Niskin bottles. The accuracy of the TA measurements on CRM (batch 117) is determined to be $0.8 \mu\text{mol kg}^{-1}$, as our results yielded a mean value of $2240.0 \mu\text{mol kg}^{-1}$, comparable to the certified value $2339.2 \mu\text{mol kg}^{-1}$. The daily drift of the system was determined by regular measurements of substandard seawater; this drift was always very low.

The DIC was analysed at GEOMAR with the same methodology and equipment as in M84/3. Precision and accuracy of measurements are the same as those reported for the M84/3 cruise, see above.

3 Consistency of CO₂ analysis

3.1 Inter-cruise consistency

A crossover analysis was performed between the M84/3 and EF11 CO₂ data using the methodology applied to the CARINA database (Tanhua et al., 2010). We studied two areas: the Tyrrhenian Sea (4 stations each cruise) and the Ionian Sea (3 stations from M84/3 and 2 from EF11) (Fig. 1). We compared the DIC, pH and TA data below 1000 dbars: DIC difference is less than $2 \mu\text{mol kg}^{-1}$ in both sites; EF11 TA is about $11 \mu\text{mol kg}^{-1}$ higher and was therefore reduced by this amount, and pH_{25T} differences are quite noisy and less than 0.01. Therefore, EF11 CO₂ data were not included in the following analysis of the internal consistency of the CO₂ system, Sect. 3.2.

Using the preferred set of constants reported on in Sect. 3.2, we compared measured DIC with that calculated from pH and TA using option 4 and the CO₂SYSTM programme for [®]MATLAB (see next section). After rejecting some outliers, the mean difference between measured and calculated DIC is $-0.4 \pm 10 \mu\text{mol kg}^{-1}$. In summary, no adjustments were done to the EF11 DIC and pH measurements, whereas the TA was reduced by $11 \mu\text{mol kg}^{-1}$ as a consequence of the comparison between M84/3 and EF11 data.

The EF11 CO₂ data will be used to discuss the CO₂ system properties in water masses of the passage between Sardinia and Sicily, Sect. Sardinia Sicily passage.

3.2 Internal consistency analysis for the CO₂ system in the MedSea

There is a wealth of literature regarding the internal consistency of CO₂ analysis in seawater and its dissociation constants, see the review by Millero (2007), but to the best of our knowledge the last study about this issue was published in 2002 compiling up to 6000 measurements from NSF/JGOFS, NOAA/OACES and DOE/WOCE cruises in the Atlantic, Pacific, Southern and Indian oceans (Millero et al., 2002), but without any CO₂ data from the MedSea.

Table 1. Mean values and standard deviation of the residuals (measured minus calculated) for alkalinity (TA), Dissolved Inorganic Carbon (DIC) and pH at the total scale and referred to 25 °C (pH25T) calculated with different thermodynamic constants for CO₂ according to the CO2SYS programme options. The sulphate constant from Dickson (1990) and total borate concentration from Khoo et al. (1977) were used in all cases.

Constants	TA	DIC	pH25T
1	-16.1 ± 4.0	14.7 ± 3.6	0.024 ± 0.005
2	-11.1 ± 3.7	10.2 ± 3.4	0.016 ± 0.005
3	-5.0 ± 3.5	4.6 ± 3.2	0.007 ± 0.005
4	0.1 ± 3.3	-0.1 ± 3.0	-0.0003 ± 0.005
5	-3.7 ± 3.5	3.4 ± 3.2	0.005 ± 0.005
6	6.3 ± 3.2	-5.9 ± 3.0	-0.009 ± 0.005
7	-3.6 ± 3.5	3.3 ± 3.2	0.005 ± 0.005
9	17.3 ± 3.2	-16.1 ± 3.0	-0.027 ± 0.005
10	0.6 ± 3.3	-0.6 ± 3.0	-0.001 ± 0.005
11	-4.3 ± 3.6	3.9 ± 3.3	0.006 ± 0.005
12	-10.2 ± 4.4	9.3 ± 4.0	0.015 ± 0.006
13	2.8 ± 3.3	-2.6 ± 3.1	-0.004 ± 0.005
14	1.5 ± 3.4	-1.4 ± 3.1	-0.002 ± 0.005

(1) Roy (1993); (2) Goyet and Poisson (1989); (3) Hansson (1973a, b) refit by Dickson and Millero (1987); (4) Mehrbach et al. (1973) refit by Dickson and Millero (1987); (5) Hansson (1973a, b) and Mehrbach et al. (1973) refit by Dickson and Millero (1987); (6) GEOSECS choice (Takahashi et al., 1982); (7) Peng et al. (1987); (9) Cai and Wang (1998); (10) Lueker et al. (2000); (11) Mojica-Prieto and Millero (2002); (12) Millero et al. (2002); (13) Millero et al. (2006); (14) Millero (2010).

Despite the lack of surface or column partial pressure CO₂ (*p*CO₂) measurements, this study presents high-quality DIC, TA and pH data covering the whole MedSea that can be used to perform the first internal consistency analysis in this area for CO₂ measurements.

By using the consensus programme for seawater CO₂ calculations CO2SYS, configured for [®]MATLAB by van Heuven et al. (2011), we tested the internal consistency of our measurements for the various CO₂ constants using all options, except that for pure water only (option 8). We also changed the sulfate constants (Dickson, 1990; Khoo, 1977) and the parameterization of borate as a function of salinity (Uppström, 1974; Lee et al., 2010). The inorganic nutrients concentrations were also taken into account.

The option yielding minimum differences between the calculated and measured variable for the three combinations (TA-pH, TA-DIC and DIC-pH) (Table 1 and Fig. 2) is obtained by using option 4 [CO₂ constants from Mehrbach et al., 1973; refitted by Dickson and Millero, 1987], the sulphate constant from Dickson (1990) and the parameterization of borate from Uppström (1974). Using this borate function and the sulphuric constant from Khoo (1977) yields practically the same results (not shown). Using option 13 (Millero et al., 2006), the more recent borate function by Lee et al. (2010) and either sulphate constant (Khoo, 1977 or Dickson, 1990) low residuals are also obtained (not shown).

By using our preferred set of constants (see above) our pH, TA and DIC measurements along the M84/3 cruise are internally consistent to -0.0003 ± 0.005 for pH, $0.1 \pm 3.3 \mu\text{mol kg}^{-1}$ for TA and $-0.1 \pm 3 \mu\text{mol kg}^{-1}$ for DIC. This combination of constants is also the preferred option in global ocean CO₂ data synthesis projects such as GLODAP (Key et al., 2004) and CARINA (Key et al., 2010). At the light of these results, the bias of 0.0962 ± 0.0012 in the pH25T measurements obtained after CRM measurements for pH during M84/3 was disregarded.

The effect of uncertainties in *p*K₁ and *p*K₂ using the pH – TA combination is identical to those observed using pH – DIC. As summarized in Lee et al. (1997) when pH and TA (pH and DIC) are used as input parameters, calculated DIC (TA) depends on *p*K₂, which is also dependent upon the DIC/TA ratio; the lower the ratio the higher the sensitivity to *p*K₂. However, only a reliable *p*K₁ is needed to calculate *p*CO₂ from the pH–TA (pH–DIC) combination; in this case the lower the DIC/TA ratio the lower the sensitivity to *p*K₁. Calculated pH from the TA–DIC input combination relies on a good estimation of *p*K₁–*p*K₂ (the K₁/K₂ ratio). The DIC/TA ratio is an indicative of the concentration of carbonates; the lower the ratio the higher the [CO₃]²⁻ concentration, which is also sensitive to *p*K₂. Lacking measured *p*CO₂ data we are not able to check the dependence on K₁ in the calculation of *p*CO₂ (pH–DIC or pH–TA inputs) or pH (*p*CO₂–DIC or *p*CO₂–TA inputs).

Having the former information in mind, a closer look at the pH, TA and DIC residuals (measured minus calculated values) reveals some insights and peculiarities about the internal consistency of CO₂ measurements in the high TA (low DIC/TA) and salinity MedSea waters. Figure 3 shows the longitudinal distribution of the residuals in the MedSea pointing to a decreasing trend eastwards for TA (Fig. 3a) and on the contrary an increasing trend eastwards for DIC and pH (Fig. 3b and c) which seem to be related with the eastwards salinity increase (Fig. 3 in Tanhua et al., 2013a), DIC/TA ratio decrease (Fig. 10h) or [CO₃]²⁻ increase. The pH residuals are a function of *p*K₁–*p*K₂, but mostly dependent on K₂, while the TA or DIC residuals are a function of *p*K₂ (Lee et al., 1997; Millero, 2007). The relation between pH and TA residuals is linear (Fig. 4), but two regression lines are detected depending on salinity. Samples with salinity higher than 36.1 have a higher slope ($-0.0015 \pm 4.5 \times 10^{-6}$, $r^2 = 0.9937$, $n = 725$) than fresher ones ($-0.0020 \pm 2.9 \times 10^{-5}$, $r^2 = 0.9945$, $n = 28$). Including measured pH, TA and DIC data from five CARINA cruises (Key et al., 2010) between the Strait of Gibraltar and 24° W and 40° N to 24° N the same tendency is detected (data with salinity < 36.1, slope = $-0.0022 \pm 8.7 \times 10^{-6}$, $r^2 = 0.9919$, $n = 671$; data with salinity ≥ 36.1, slope = $-0.0016 \pm 6.7 \times 10^{-6}$, $r^2 = 0.9977$, $n = 182$). This result points to the need for a revision of the K₂ parameterization for waters with high salinity and low DIC/TA ratio, as in the MedSea, as the CO₂ chemistry is more sensitive to K₂.

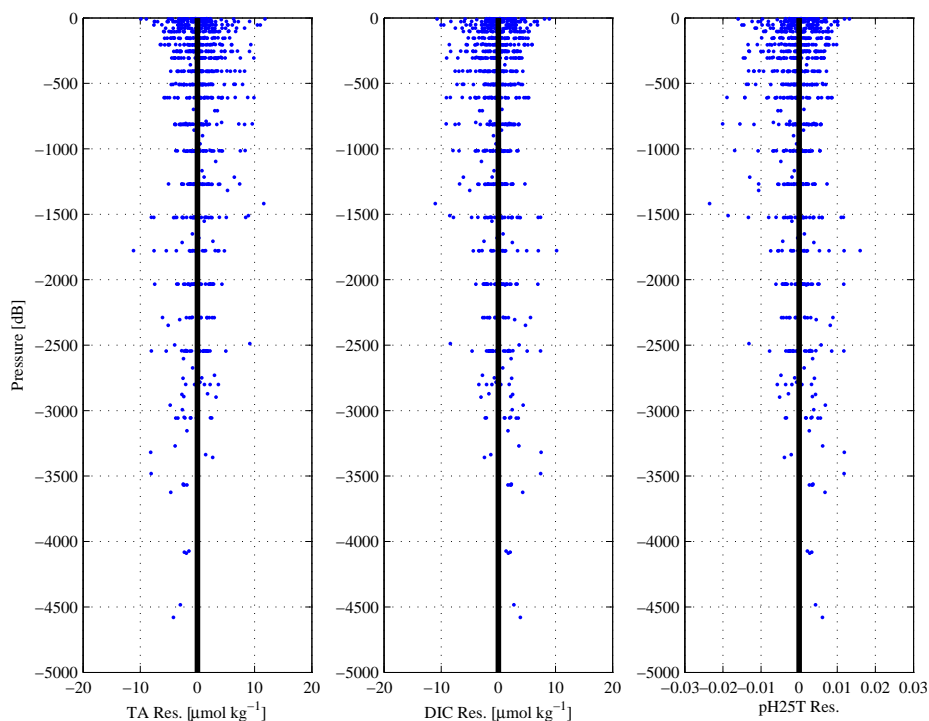


Fig. 2. Vertical distribution of the residual (measured minus calculated) values for TA ($\mu\text{mol kg}^{-1}$), DIC ($\mu\text{mol kg}^{-1}$) and pH_{25T} using option 4 in CO₂SYS, see Table 1.

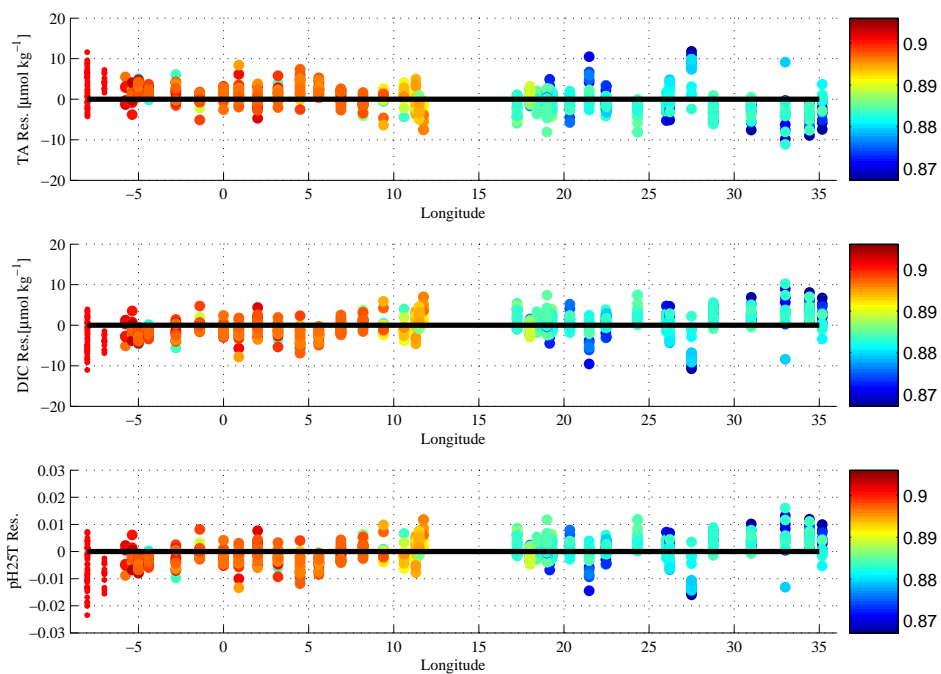


Fig. 3. Same as in Fig. 2 but plotted vs. longitude. The colour code corresponds to the DIC/TA ratio. Two stations to the west of the Strait of Gibraltar were coded as red because DIC/TA ratio > 0.94 .

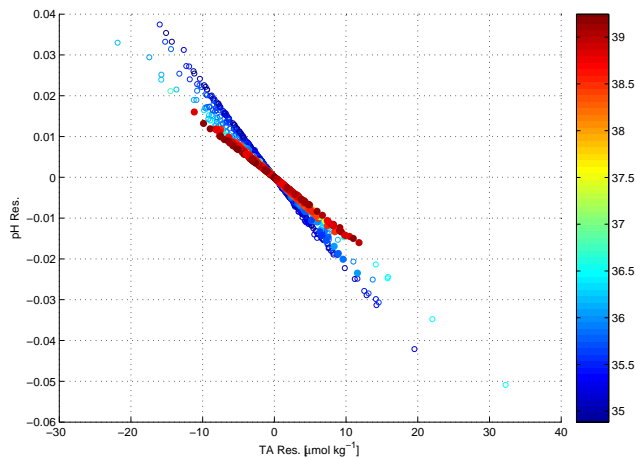


Fig. 4. Relationship between the TA and pH25T residuals for the M84/3 data (filled symbols) and some CARINA cruises (open symbols). The colour code stands for salinity.

In summary, the preferred option for CO₂ constants for global studies on internal consistency (CO₂ constants from Mehrbach et al., 1973; refitted by Dickson and Millero, 1987; sulphate constant from Dickson, 1990; total borate from Upström, 1974) also applies for MedSea waters. However, further studies are needed, with an additional fourth measurement, either $p\text{CO}_2$ or $[\text{CO}_3]^{2-}$ (Byrne and Yao, 2008) to confirm the internal consistency of K_1 and K_2 with the measurements in the peculiar MedSea waters.

4 Distribution of CO₂ species in the Mediterranean Sea

The general aim of this section is to provide a large-scale distribution of measured and derived CO₂ properties along the full length of the Mediterranean Sea and corresponding sub-basins, being complementary to the physical (temperature and salinity) and chemical (dissolved oxygen and inorganic nutrients) variables presented by Tanhua et al. (2013a). Water mass characterisation will be commented using vertical distributions and property-property plots for the different sub-basins.

4.1 Vertical distributions

4.1.1 Measured variables

Meteor M84/3 cruise data

Vertical distributions of TA (Fig. 5), DIC (Fig. 6) and pH25T (Fig. 7) clearly distinguish several water masses in the MedSea, from surface to bottom:

- i. Levantine Surface Water (LSW): this water formed by intensive heating and evaporation, has the largest salinity and temperature of the entire MedSea ($> 17^\circ\text{C}$,

> 38.9), clearly seen in the surface layer of the Levantine Basin (Tanhua et al., 2013a). LSW has TA values around $2610 \mu\text{mol kg}^{-1}$, DIC around $2270 \mu\text{mol kg}^{-1}$ and pH25T around 8.03 (Figs. 5–7).

- ii. Atlantic Water (AW): enters through the Strait of Gibraltar and flows eastward, it is mainly detected by a low salinity signal in the upper 50–100 dbars (Fig. 3 in Tanhua et al., 2013a) from the Strait of Gibraltar to the Levantine Basin (36.2–38.9). AW is also characterised by a low TA signal evolving from values $< 2560 \mu\text{mol kg}^{-1}$ in the western basin to $< 2600 \mu\text{mol kg}^{-1}$ in the Levantine Basin and Ionian Sea (Fig. 5). The same trend was seen in DIC evolving from $2250 \mu\text{mol kg}^{-1}$ in the western to $2270 \mu\text{mol kg}^{-1}$ in the Levantine Basin (Fig. 6), pH25T increased from 8 to 8.014 eastwards (Fig. 7).

The MedSea is considered one of the most oligotrophic areas in the world (Azov, 1991) with low phytoplankton biomass and primary production decreasing eastward, confirmed by in situ measurements (Ignatiades et al., 2009; Moutin and Raimbalut, 2002; Siokou-Frangou et al., 2010), satellite data (Bosc et al., 2004; Volpe et al., 2007; D’Ortenzio and Ribera d’Alcalà, 2009) and modelling studies (Crise et al., 1999; Lazzari et al., 2012). The period of the M84/3 cruise, April, coincides with the end of the winter-spring bloom (D’Ortenzio and Ribera d’Alcalà, 2009; Lazzari et al., 2012). Surface Chlorophyll *a* (Chl *a*) and primary production data during the M84/3 cruise were presented in Rahav et al. (2013) with a clear westward increasing gradient, and values ranging from 0 to $0.4 \mu\text{g L}^{-1}$ for Chl *a*, and 0.2 to $15 \mu\text{gCL}^{-1} \text{d}^{-1}$ for primary production.

The gathered biogeochemical data during the M84/3 cruise showed that the upper 50 dbars are supersaturated in oxygen ($\text{AOU} < 0$) with more negative values in the western basin where higher primary production was reported (Rahav et al., 2013). While in the western basin inorganic nutrients were still available, in the eastern basin they were depleted, especially phosphate (see corresponding figures in Tanhua et al., 2013a). For waters with pressure < 60 dbars, there was no clear relationship between AOU and either DIC, TA or pH25T, except in the western basin where pH25T related with AOU ($\text{pH25T} = -0.0015 \pm 0.00008 \cdot \text{AOU} + 7.97 \pm 0.001$, $r^2 = 0.83$ $p < 0.001$), pointing to a pH modulation by primary production.

- iii. Levantine Intermediate Water (LIW): this warm and high salinity water is formed in the Levantine Basin, mainly in the Rhodes Gyre area. During the M84/3 cruise LIW was clearly detected by the salinity maximum around 200 dbars in the eastern basin (Tanhua et al., 2013a), with TA $> 2620 \mu\text{mol kg}^{-1}$,

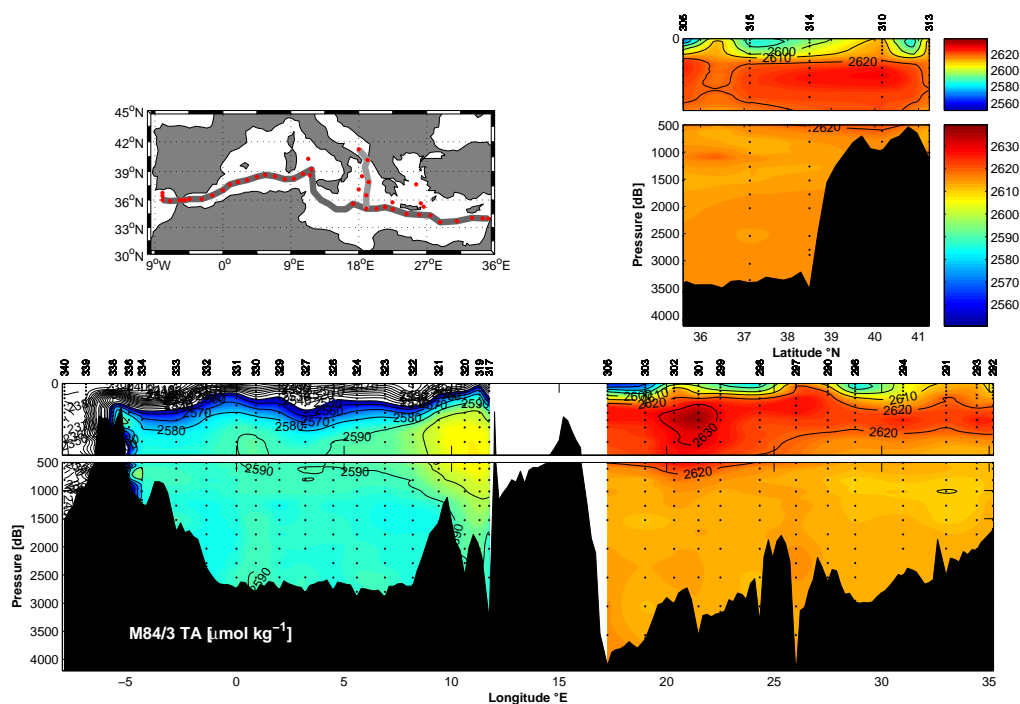


Fig. 5. Sections of TA ($\mu\text{mol kg}^{-1}$) in the Mediterranean Sea from the Meteor cruise M84/3 in April of 2011. The top right panel is a meridional section from the Adriatic Sea to the Ionian Sea (light gray line on the map) and the lower panel is the zonal section from the coast of Lebanon in the Eastern Mediterranean Sea to through the Strait of Gibraltar (dark gray line on the map). The depth scale and the colour scale are identical all both panels. The top 500 dbars in each section are slightly expanded. No stations are shown in the Atlantic due to the very different TA encountered there as compared to the Mediterranean Sea.

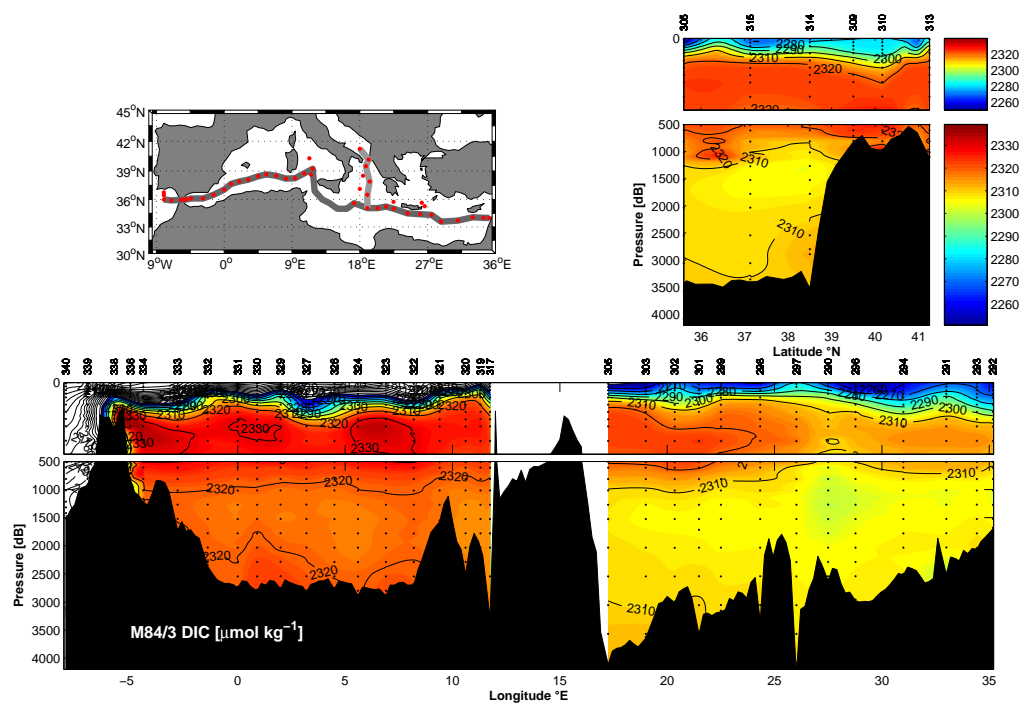


Fig. 6. As in Fig. 5 but for DIC ($\mu\text{mol kg}^{-1}$).

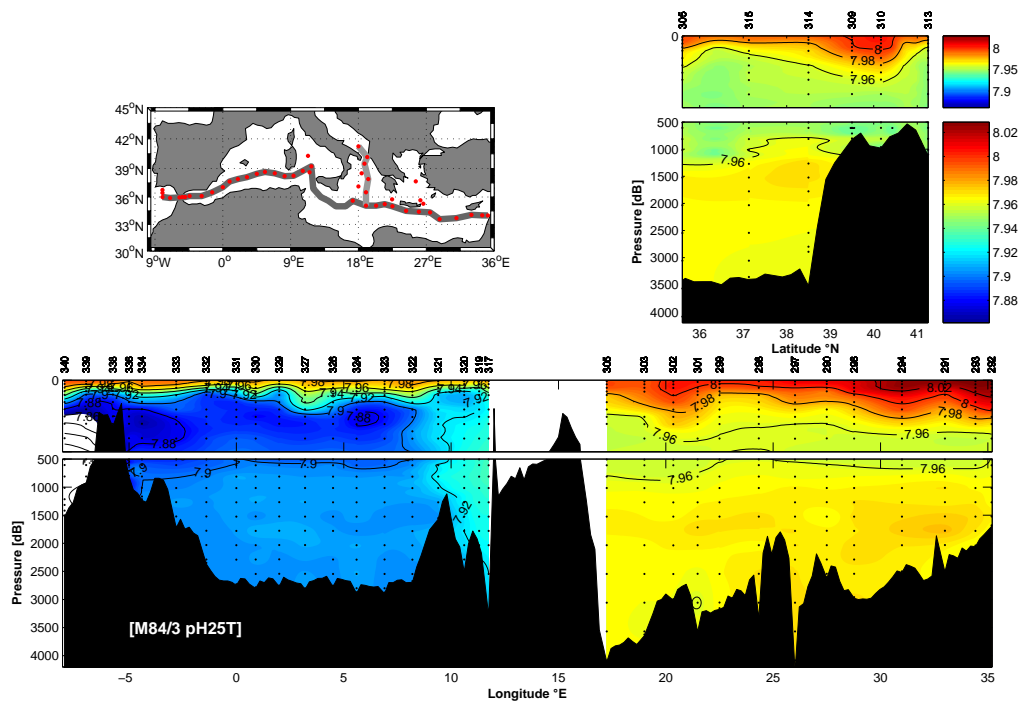


Fig. 7. As in Fig. 5 but for pH25T.

DIC > 2310 $\mu\text{mol kg}^{-1}$, but no clear signal in pH which varies between 7.96 and 7.98 (Figs. 5, 6 and 7). In the western basin LIW was found around 500 dbars as a maximum in salinity, corresponding to TA ($\approx 2590 \mu\text{mol kg}^{-1}$) (Fig. 5), maximum in DIC ($\approx 2330 \mu\text{mol kg}^{-1}$) (Fig. 6) and minimum pH25T (≈ 7.9) (Fig. 7). In the eastern basin, the maximum layer of remineralization, indicated by the oxygen minimum (see Fig. 6 in Tanhua et al., 2013a), was located below LIW while in the western basin, both coincided.

- iv. Eastern Mediterranean Deep Water (EMDW): along the M84/3 cruise track in the eastern MedSea three types of EMDW could be distinguished mainly using salinity and AOU (Tanhua et al., 2013a) and tracers such as CFC-12 (Stöven and Tanhua, 2013). Around 1000 dbar in the Levantine Basin a layer with higher salinity and AOU maxima related with pre-EMT-EMDW with an Adriatic Sea origin. In this basin, below 1500 dbars a more saline water and higher in oxygen pointed to EMDW with an Aegean Sea origin produced during the EMT, although more mixed compared to that found in the Ionian Sea. Here salinity and AOU were lower. The third EMDW is that found in the near-bottom layer of the Ionian Sea, it was produced after the EMT (> 2001) and has an Adriatic Sea origin (Hainbucher et al., 2013).

The upper panels in Figs. 5, 6 and 7 show the distribution of CO₂ species from the centre of the Ionian Sea to the Adriatic Pit. Here, below 3000 dbars, salinity increased in about 0.01 units (not shown), and TA as well (not resolved by the contour or the colour scale in Fig. 5) and DIC (Fig. 6) increased towards the bottom by about 4 $\mu\text{mol kg}^{-1}$. Correspondingly, pH25T decreased by about 0.002 (note the greenish colour in the bottom of the upper panel in Fig. 7). The tracers distributions, CFC-12 and SF₆ (Stöven, 2011), also increased towards the bottom. These results point to a recent arrival of EMDW formed in the Adriatic Sea as commented previously.

- v. Western Mediterranean Deep Water (WMDW): being fresher and colder than EMDW, the deep layers below 1500 dbars in the western MedSea during M84/3 were quite homogeneous in the physical (potential temperature and salinity) properties. A closer look showed two distinct WMDW varieties: a younger one, close to the bottom, as noted by the CFC-12 distribution (Stöven, 2011) and saltier than the older WMDW, immediately above 2000 dbars (Hainbucher et al., 2013). Bottom (younger) WMDW also had higher DIC values by about 7 $\mu\text{mol kg}^{-1}$, lower pH25T values by about 0.004, and higher TA values by about 4 $\mu\text{mol kg}^{-1}$, i.e. within the accuracy limits of the latter two variables (Figs. 5–7).

An outstanding feature in the vertical distribution of CO₂ variables was the pH_{25T} minimum (Fig. 7) around 500 dbars in the Levantine and Ionian basins. In the Levantine basin this minimum was coincident with the oxygen minimum (Fig. 6 in Tanhua et al., 2013a) and a DIC maximum (Fig. 6). Whereas in the Ionian Sea the pH_{25T} minimum/DIC maximum (500 dbars) was shallower than the oxygen minimum that was situated around 1000 dbars. All these extreme layers differ from the LIW layer, the salinity maximum was shallower in both basins, Levantine and Ionian. However, in the western basin, the LIW signal was coincident with the layer of highest remineralization as indicated by the DIC maxima and the oxygen/pH_{25T} minimum.

During the M84/3 cruise we sampled the interior of the Tyrrhenian Sea: in the upper layer low salinity (Tanhua et al., 2013a) and TA values (Fig. 5) pointed to AW. Around 400 dbars the maximum in salinity, TA, DIC and pH_{25T} (Figs. 5, 6 and 7) were associated with LIW entering through the Sicily channel; Tyrrhenian Deep Water (TDW) formed from the mixing of LIW and WMDW was detected below the TA maximum associated with LIW and bottom water with lower TA and pH_{25T} and higher DIC values (Figs. 5, 6 and 7). This bottom water corresponds to WMDW that has started to cascade into the Tyrrhenian Sea from the western basin in 2011, also higher in tracer concentrations (Stöven and Tanhua, 2013).

As a reference for future studies and calculations in Sect. 4.1.2, Table 2 shows the mean values and standard deviation for salinity and different CO₂ species in the MedSea sub-basins and Atlantic waters west of the Strait of Gibraltar as sampled in 2011 during the Meteor M84/3 cruise by different depth intervals.

The direct comparison of our CO₂ data with previously published CO₂ data, either DIC, TA or pH, in order to identify and quantify trends is out of the scope of our manuscript. The available data for CO₂ variables in the MedSea is quite heterogeneous (see review in Álvarez, 2012, and below). A detail study about CO₂ temporal changes in the interior MedSea will be the aim of a forthcoming work. We do however make a rough comparison in order to detect possible biases in the historic dataset as compared to ours and vice versa. Qualitatively, our TA and DIC data in the western MedSea seems to be 5–10 and 40–70 μmol kg⁻¹ lower, respectively, than those shown in Millero et al. (1979) from a cruise in 1976. This result is counterintuitive due to the expected increase in DIC due to input of anthropogenic carbon (C_{ANT}). However, the data from Millero et al. (1979) originates before the use of certified reference materials (CRMs), so that the accuracy of these early data can be questioned. Our TA and DIC are however more comparable to those from the Almofront cruise in 1991 (Copin-Montegut, 1993). The data shown by Touratier and Goyet (2009) from the DYFAMED site in the Ligurian Sea below 1000 dbar, corresponding to WMDW, are lower than our WMDW values by about 5 μmol kg⁻¹ for both DIC and TA.

The reference cruise for the CO₂ system in the eastern and part of the western MedSea is the M51/2 cruise (R/V Meteor 2001) available at CDIAC; the TA data was presented in Schneider et al. (2007) and the DIC in Schneider et al. (2010). The TA data are comparable, but our DIC are roughly 10 μmol kg⁻¹ higher, which could be a real signal considering the 10 yr between the measurements and the uptake of anthropogenic carbon.

The VECTOR cruise in 2007 sampled 8 stations in the eastern and western MedSea for pH and TA, whereas DIC was calculated (Rivaro et al., 2010). Examining data from the western basin below 700 dbars, the TA data are comparable to each other whereas the DIC and pH values reported by Rivaro et al. (2010) are higher than ours by 10 μmol kg⁻¹ and by 0.01, respectively. In the eastern basin, our data below 700 dbars for pH and TA are comparable but our DIC seems 20 μmol kg⁻¹ higher. More recent CO₂ data are reported from the BOUM cruise in 2008 (Pujo-Pay et al., 2011; Touratier and Goyet, 2012); their DIC data seem higher than ours by about 10 μmol kg⁻¹ in both the eastern and western basins.

Sardinia Sicily passage

The vertical distributions of physical properties in the Sardinia Sicily passage, already analysed in the last decade of last century (Astraldi et al., 2002), indicate that the passage is a crucial chokepoint where almost all MedSea waters can be intercepted (see the review by Astraldi et al., 2002). The Sardinia Sicily transect, for its local character, was not included in the overall MedSea description done by Tanhua et al. (2013a). The main water masses crossing the passage have been identified according to their physical characteristics using potential temperature and salinity (Fig. 8a and b), AOU, (Fig. 8c) and CO₂ variables (Fig. 8d–f). On the eastern part (close to Sicily) only inflowing waters can be observed, from surface to bottom: (1) a fresh vein of AW (0–200 dbars), coming directly from Gibraltar through the Algerian sub-basin, was evident from the low salinity (\ll 38.00) (Fig. 8b) and supported by the lowest TA values (2525–2575 μmol kg⁻¹) (Fig. 8d); this inflowing AW was not in equilibrium with atmospheric oxygen (AOU between 20–40 μmol kg⁻¹, Fig. 8c), pH_{25T} (\approx 7.950, Fig. 8f) and DIC values (2225–2285 μmol kg⁻¹, Fig. 8e) were the lowest observed along the Sect. 2) Below AW, the inflow of the saltiest water ($>$ 38.75) in the transect, LIW, coming from the eastern MedSea, after crossing the Sicily Channel, the high AOU (50–60 μmol kg⁻¹) and DIC (\approx 2300 μmol kg⁻¹) values aside of the low pH_{25T} ($<$ 7.940) highlight the organic matter remineralization processes occurring within the LIW; TA values as high as 2605–2610 μmol kg⁻¹ were observed. (3) Below LIW, there was a thin layer of dense transitional Eastern Mediterranean Deep Water (tEMDW, i.e. the upper layer of the deep water filling the Eastern Mediterranean, which is able to cross the channel); tEMDW is cooler and

Table 2. Mean values and standard deviation for salinity and CO₂ species in the different MedSea sub-basins and west of the Strait of Gibraltar as sampled during the M84/3 cruise. Several vertical intervals are considered: surface (0–150 dbars in the East and 0–200 dbars in the West MedSea), intermediate (East: 150–500 and West: 200–500 dbars), deep (East: 500–2500 and West: 600–2000 dbars) and bottom (East: > 2500 and West: > 2000 dbars). IS stands for in situ values. Ar stands for aragonite and Ca for calcite.

SURFACE	Salinity	TA $\mu\text{mol kg}^{-1}$	DIC $\mu\text{mol kg}^{-1}$	pH25T	CO ₂ IS $\mu\text{mol kg}^{-1}$	Ω -Ar IS	Ω -Ca IS
Aegean	39.20 ± 0.01	2628 ± 2	2291 ± 4	8.009 ± 0.006	13.1 ± 0.2	3.7 ± 0.1	5.6 ± 0.1
Levantine	39.05 ± 0.13	2612 ± 10	2277 ± 15	8.010 ± 0.017	13.1 ± 0.6	3.6 ± 0.1	5.5 ± 0.2
Ionian	38.73 ± 0.21	2607 ± 16	2289 ± 17	7.985 ± 0.015	13.5 ± 0.6	3.4 ± 0.1	5.1 ± 0.2
Adriatic	38.70 ± 0.12	2616 ± 1	2298 ± 16	7.980 ± 0.023	14.0 ± 0.9	3.5 ± 0.2	5.3 ± 0.2
Tyrrhenian	38.32 ± 0.29	2570 ± 26	2294 ± 32	7.929 ± 0.021	16.2 ± 1.0	3.1 ± 0.1	4.7 ± 0.2
Western	37.79 ± 0.51	2522 ± 46	2250 ± 54	7.930 ± 0.033	15.9 ± 1.6	3.0 ± 0.2	4.6 ± 0.2
Atlantic	36.75 ± 0.89	2423 ± 83	2166 ± 83	7.927 ± 0.038	14.6 ± 1.7	2.7 ± 0.2	4.1 ± 0.3
INTERM.	Salinity	TA $\mu\text{mol kg}^{-1}$	DIC $\mu\text{mol kg}^{-1}$	pH25T	CO ₂ IS $\mu\text{mol kg}^{-1}$	Ω -Ar IS	Ω -Ca IS
Aegean	39.14 ± 0.02	2636 ± 2	2318 ± 8	7.975 ± 0.01	14.3 ± 0.4	3.4 ± 0.1	5.1 ± 0.2
Levantine	39.04 ± 0.11	2621 ± 4	2310 ± 10	7.970 ± 0.016	14.6 ± 0.6	3.3 ± 0.1	5.0 ± 0.2
Ionian	39.00 ± 0.08	2627 ± 6	2321 ± 5	7.962 ± 0.012	14.9 ± 0.5	3.3 ± 0.1	5.0 ± 0.2
Adriatic	38.79 ± 0.13	2620 ± 6	2320 ± 7	7.954 ± 0.015	15.2 ± 0.6	3.2 ± 0.1	4.9 ± 0.2
Tyrrhenian	38.70 ± 0.03	2603 ± 3	2324 ± 2	7.926 ± 0.005	16.4 ± 0.3	3.0 ± 0.1	4.5 ± 0.1
Western	38.50 ± 0.08	2586 ± 8	2326 ± 7	7.892 ± 0.010	17.7 ± 0.5	2.8 ± 0.1	4.2 ± 0.1
Atlantic	36.03 ± 0.66	2372 ± 55	2172 ± 42	7.828 ± 0.038	19.7 ± 1.7	2.2 ± 0.2	3.4 ± 0.3
DEEP	Salinity	TA $\mu\text{mol kg}^{-1}$	DIC $\mu\text{mol kg}^{-1}$	pH25T	CO ₂ IS $\mu\text{mol kg}^{-1}$	Ω -Ar IS	Ω -Ca IS
Aegean	39.05 ± 0.02	2633 ± 2	2323 ± 2	7.964 ± 0.003	14.5 ± 0.2	2.7 ± 0.2	4.1 ± 0.4
Levantine	38.78 ± 0.02	2613 ± 2	2306 ± 3	7.967 ± 0.004	14.5 ± 0.3	2.7 ± 0.2	4.1 ± 0.4
Ionian	38.77 ± 0.06	2615 ± 3	2309 ± 5	7.965 ± 0.004	14.6 ± 0.3	2.8 ± 0.2	4.2 ± 0.3
Adriatic	38.75 ± 0.04	2618 ± 3	2326 ± 5	7.940 ± 0.008	15.6 ± 0.3	2.9 ± 0.1	4.4 ± 0.2
Tyrrhenian	38.57 ± 0.05	2595 ± 5	2318 ± 2	7.923 ± 0.008	16.3 ± 0.3	2.6 ± 0.2	3.8 ± 0.2
Western	38.48 ± 0.01	2587 ± 2	2319 ± 2	7.906 ± 0.003	16.6 ± 0.2	2.5 ± 0.1	3.7 ± 0.2
Atlantic	36.10 ± 0.25	2390 ± 16	2201 ± 6	7.795 ± 0.026	21.0 ± 1.0	1.9 ± 0.1	2.9 ± 0.2
BOTTOM	Salinity	TA $\mu\text{mol kg}^{-1}$	DIC $\mu\text{mol kg}^{-1}$	pH25T	CO ₂ IS $\mu\text{mol kg}^{-1}$	Ω -Ar IS	Ω -Ca IS
Aegean	–	–	–	–	–	–	–
Levantine	38.75 ± 0.01	2613 ± 2	2308 ± 1	7.969 ± 0.001	12.9 ± 0.2	2.0 ± 0.2	2.9 ± 0.3
Ionian	38.73 ± 0.001	2615 ± 2	2310 ± 2	7.965 ± 0.003	14.3 ± 0.1	2.1 ± 0.2	3.1 ± 0.3
Adriatic	–	–	–	–	–	–	–
Tyrrhenian	38.51 ± 0.01	2589 ± 3	2317 ± 1	7.916 ± 0.005	16.3 ± 0.2	2.1 ± 0.1	3.1 ± 0.2
Western	38.48 ± 0.001	2587 ± 2	2321 ± 2	7.906 ± 0.002	16.7 ± 0.1	2.1 ± 0.1	3.1 ± 0.1
Atlantic	–	–	–	–	–	–	–

fresher than LIW ($< 13.8^\circ\text{C}$ and < 38.65), as well as for the higher DIC, TA (2318 and $2612 \mu\text{mol kg}^{-1}$, respectively, Fig. 8d and e) and inorganic nutrient values (not shown) and the lower pH25T (< 7.930 , Fig. 8f); given its high density tEMDW cascades at greater depths to the interior of the Tyrrhenian Sea, contributing to the formation of the Tyrrhenian Deep Water, TDW, and provoking an intense mixing that dilutes its original physical properties (tEMDW is significantly warmer and saltier than TDW), in contrast the chemical properties of these two deep water masses remain very similar (Fig. 8).

On the western part (close to Sardinia) there are both inflowing and outflowing water masses, from surface to bottom: (1) close to Sardinia the outflowing AW has

circulated through the Tyrrhenian Sea, becoming saltier ($38.00 < \text{salinity} < 38.20$, note the depth decrease towards Sardinia of the 38 isoline, Fig. 8b) and even less saturated in oxygen (AOU $35\text{--}40 \mu\text{mol kg}^{-1}$, note the depth decrease towards Sardinia of the 20 isoline, Fig. 8c) than the inflowing AW on the Sicilian side; CO₂ variables are also slightly different ($2550 < \text{TA} < 2575 \mu\text{mol kg}^{-1}$; $2270 < \text{DIC} < 2285 \mu\text{mol kg}^{-1}$; $7.940 < \text{pH25T} < 7.950$, note the sloping isolines in Fig. 8d–f). (2) Below the outflowing AW, an outflowing LIW vein can be noted, which in turn, after its path through the whole Tyrrhenian Sea has become colder ($\approx 14.0^\circ\text{C}$) and less salty (< 38.68) than the inflowing LIW on the eastern edge of the section, due to the mixing; this fact also lowers TA ($\approx 2600 \mu\text{mol kg}^{-1}$,

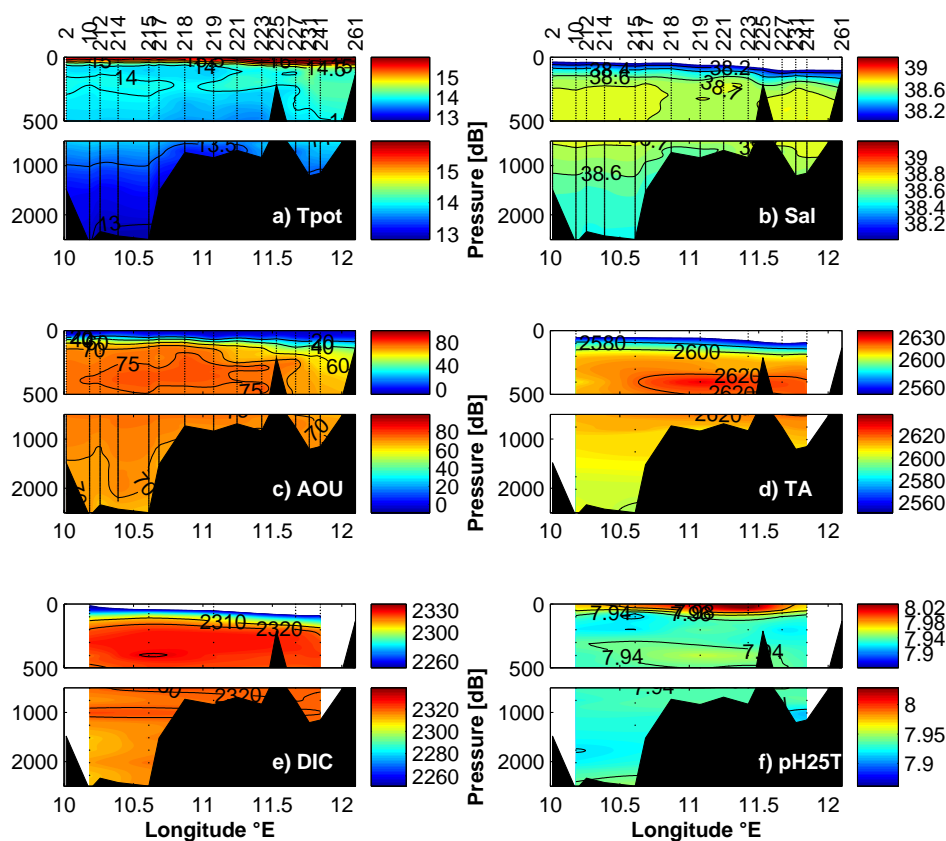


Fig. 8. Vertical distributions across the Sardinia Sicily passage using EF11 data of (a) potential temperature (°C), (b) salinity, (c) Apparent Oxygen Utilisation (AOU, $\mu\text{mol kg}^{-1}$), (d) TA ($\mu\text{mol kg}^{-1}$) (e) DIC ($\mu\text{mol kg}^{-1}$) and (f) pH_{25T}. Potential temperature, salinity and AOU are derived from CTD data, CTD-oxygen was calibrated with bottle data.

Fig. 8d) and increases DIC ($\approx 2310 \mu\text{mol kg}^{-1}$, Fig. 8e) while the pH_{25T} (Fig. 8f) remains similar; outflowing LIW is also characterised by an absolute AOU maximum ($65 < \text{AOU} < 73 \mu\text{mol kg}^{-1}$, Fig. 8c) due to ageing. (3) In the central part of passage, over the plateau, there is an inflow of “old LIW” (Astraldi et al., 2002) (identified by its salinity maximum, but less salty than the outflowing LIW), also identified by higher AOU ($55\text{--}70 \mu\text{mol kg}^{-1}$, Fig. 8c) than the inflowing LIW ($50\text{--}60 \mu\text{mol kg}^{-1}$), while differences in CO₂ variables cannot be distinguished. (4) In deep layers (600–1900 dbars) the properties of LIW progressively become those of TDW, exiting the Tyrrhenian Sea, pH_{25T} show the lowest values (< 7.930 , Fig. 8f), AOU and DIC the highest ones ($72 < \text{AOU} < 74 \mu\text{mol kg}^{-1}$; $2315 < \text{DIC} < 2320 \mu\text{mol kg}^{-1}$, Fig. 8c and e) and TA values ($> 2605 \mu\text{mol kg}^{-1}$, Fig. 8d) are not particularly characterising. (5) At the bottom and squeezed on the eastern wall in the deep canyon, there is an inflowing vein of Western Mediterranean Deep Water, which can be distinguished from the TDW because is fresher (< 38.52) and colder ($< 13.4^\circ\text{C}$), has slightly lower AOU ($< 70 \mu\text{mol kg}^{-1}$), higher pH_{25T}

values (> 7.940) but similar DIC ($> 2318 \mu\text{mol kg}^{-1}$) and TA ($2605\text{--}2610 \mu\text{mol kg}^{-1}$) values.

4.1.2 Derived variables

We used measured TA, DIC and inorganic nutrients data to calculate the degree of saturation (Ω) for calcite and aragonite using the preferred set of constants (see Sect. 3.2). The whole MedSea is supersaturated ($\Omega \gg 1$) with respect to both calcite and aragonite throughout the whole water column. Figure 9 shows the vertical distribution of Ω , a clear longitudinal gradient is evident for surface, intermediate and deep waters with increasing values eastwards and a clear separation between the western, eastern MedSea basins and Atlantic waters to the west of the Strait of Gibraltar. The Ω values reported here compare well with those found by Millero et al. (1979) and Schneider et al. (2007). According to the classification by Kleypas et al. (1999) only the eastern basin in the upper 200 dbars presents adequate to optimal conditions for the development of coral reefs with $\Omega\text{-Ar} > 3.5$.

Several projects, finished (e.g. EPOCA) or on going (e.g. BIOACID, MedSeA), try to decipher the combined effect of acidification and warming on the highly adapted MedSea

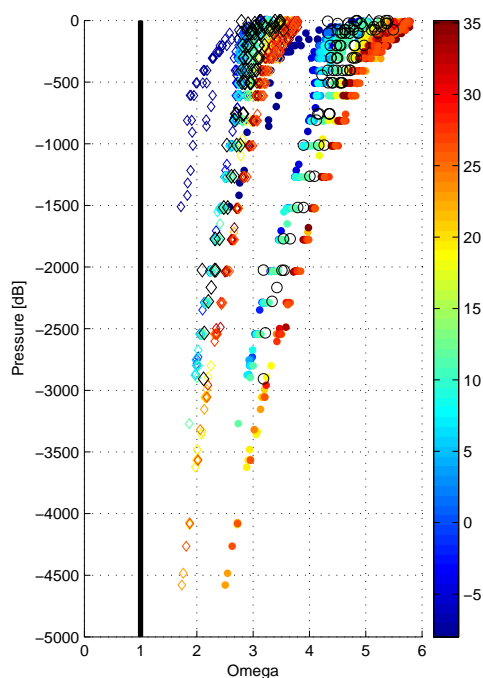


Fig. 9. Vertical distribution of the carbonate saturation state for calcite (circles) and aragonite (diamonds). Data from the EF11 cruise are shown as black circles (saturation of calcite) and diamonds (aragonite). The colour code stands for longitude.

calcareous and non-calcareous organisms. As a result of being too small and too complex in its circulation and biogeochemistry, the MedSea is usually not included in global projections models (e.g. Ricke et al., 2013) and a specific ocean-biogeochemistry model needs to be used. Here we provide a basin wide perspective for the CO₂ chemistry in the MedSea as a basis for future studies and projections.

In order to quantify the ability of MedSea waters to resist changes in the CO₂ system we calculated the buffer factors formulated by Egleston et al. (2010). The six factors proposed in their Table 1 quantify the sensitivity of aqueous CO₂ [CO₂] (γ_i), protons [H⁺] (β_i) and the carbonate saturation state Ω (ω_i) to changes in DIC and TA (subindex i) when the other parameter is kept constant. The calculations were performed with the output from CO2SYS at in situ conditions with the preferred set of constants and measured DIC and TA as inputs. The buffer factors have dimensions of mol kg⁻¹ × 10⁻³ of seawater (mmol kg⁻¹ hereinafter). See the formulation in Table 3 as several editing errors were detected in the original equations from Egleston et al. (2010).

The buffer factors γ_i express the fractional change in CO₂ when DIC changes at constant TA (air-sea CO₂ exchange) or when TA changes at constant DIC (additions of strong acid or base). The traditional Revelle factor, R , is directly calculated as $R = \text{DIC}/\gamma_{\text{DIC}}$. The buffer factor β_{TA} expresses the fractional change in hydrogen ion concentration or activity when TA changes at constant DIC (addition of a strong base or

acid). The factor β_{DIC} is identical to $-\gamma_{\text{TA}}$. Since [Ca²⁺] and the solubility products of carbonate are invariant to DIC and TA changes, the buffer factors ω_i account for the fractional change in [CO₃²⁻] when DIC or TA changes when correspondingly TA or DIC is constant. A natural process just inducing strong acid/base additions is difficult to imagine, but a cargo disaster could be possible, unfortunately. A change in natural processes (primary production/remineralization of organic matter, formation/dissolution of carbonates, freshwater balance) usually affect both TA and DIC and therefore, the sensitivity of [CO₂], pH and [CO₃²⁻] to a change in those processes can be calculated using a combination of buffer factors (Egleston et al., 2010).

The values of γ_{DIC} and β_{DIC} are positive while ω_{DIC} is negative because adding CO₂ to seawater increases [CO₂] and [H⁺] but decreases [CO₃²⁻]. Likewise, γ_{TA} and β_{TA} are negative while ω_{TA} is positive because adding a strong base to seawater decreases [CO₂] and [H⁺] but increases [CO₃²⁻]. Low buffer values imply low buffering capacity for a given change in DIC or TA. Minimum absolute values for the six buffer factors are found in waters with similar DIC and TA (DIC/TA ratio ≈ 1) and pH of about 7.5.

The six buffer factors, R and the DIC/TA ratio are shown in Fig. 10 and their mean values by sub-basin in Table 3. As the DIC/TA ratio approaches one the buffer capacities are reduced since [CO₂] is more sensitive to temperature changes at this DIC/TA ratio. From the vertical distributions in Fig. 10 we can conclude that:

- The DIC/TA ratio decreased eastwards in the MedSea; being low compared to Atlantic waters. The highest ratios, i.e. higher [CO₂] sensitivity to temperature, were associated with the Mediterranean Overflow, DIC/TA ratio > 0.9 (Fig. 10h).
- The absolute values of the buffer factors increased eastwards in the MedSea, therefore, the CO₂ system in the eastern basin is less sensitive to changes in DIC and/or TA than the western basin. Atlantic waters, to the west of the Strait of Gibraltar, would be more sensitive than waters in the MedSea.
- The absolute buffering capacities distribute as $|\omega_{\text{DIC}}| > \omega_{\text{TA}} > |\beta_{\text{TA}}| > (\beta_{\text{DIC}} = -\gamma_{\text{TA}}) > \gamma_{\text{DIC}}$. That is, the sensitivity of CO₂ concentration to changes in DIC at constant TA (air-sea CO₂ exchange) is the highest, followed by the change in pH due to the air-sea CO₂ exchange (equivalent to the change in CO₂ due to a strong acid/base addition), then changes in pH due to strong acid/base additions. Being $|\omega_{\text{DIC}}|$ and ω_{TA} the highest buffer values means that MedSea waters are able to buffer changes in the saturation state due to additions of a strong acid or base and the air-sea CO₂ exchange more easily than Atlantic waters.

Table 3. Mean values and standard deviation of several buffer factors in the different MedSea sub-basins and west of the Strait of Gibraltar as sampled during the M84/3 cruise. Same vertical intervals as in Table 2. The buffer factors have units of mmol kg⁻¹ and Revelle is dimensionless.

SURFACE	γ_{DIC}	β_{DIC}	ω_{DIC}	γ_{TA}	β_{TA}	ω_{TA}	Revelle
Aegean	0.23 ± 0.01	0.28 ± 0.01	-0.37 ± 0.01	-0.28 ± 0.01	-0.31 ± 0.01	0.35 ± 0.01	9.9 ± 0.1
Levantine	0.23 ± 0.01	0.28 ± 0.01	-0.36 ± 0.01	-0.28 ± 0.01	-0.31 ± 0.01	0.35 ± 0.01	9.9 ± 0.2
Ionian	0.22 ± 0.01	0.26 ± 0.01	-0.34 ± 0.01	-0.26 ± 0.01	-0.29 ± 0.01	0.32 ± 0.01	9.8 ± 0.2
Adriatic	0.23 ± 0.01	0.27 ± 0.01	-0.35 ± 0.01	-0.27 ± 0.01	-0.30 ± 0.01	0.33 ± 0.01	10.2 ± 0.3
Tyrrhenian	0.21 ± 0.01	0.25 ± 0.01	-0.31 ± 0.01	-0.25 ± 0.01	-0.27 ± 0.01	0.30 ± 0.01	10.8 ± 0.2
Western	0.21 ± 0.01	0.25 ± 0.01	-0.31 ± 0.01	-0.25 ± 0.01	-0.27 ± 0.01	0.29 ± 0.01	10.8 ± 0.4
Atlantic	0.19 ± 0.01	0.22 ± 0.01	-0.27 ± 0.02	-0.22 ± 0.01	-0.24 ± 0.01	0.26 ± 0.02	10.3 ± 0.4
INTERM.	γ_{DIC}	β_{DIC}	ω_{DIC}	γ_{TA}	β_{TA}	ω_{TA}	Revelle
Aegean	0.23 ± 0.01	0.28 ± 0.01	-0.35 ± 0.01	-0.28 ± 0.01	-0.30 ± 0.01	0.33 ± 0.01	10.2 ± 0.1
Levantine	0.22 ± 0.01	0.27 ± 0.01	-0.34 ± 0.01	-0.27 ± 0.01	-0.30 ± 0.01	0.33 ± 0.01	10.3 ± 0.2
Ionian	0.22 ± 0.01	0.27 ± 0.01	-0.34 ± 0.01	-0.27 ± 0.01	-0.29 ± 0.01	0.32 ± 0.01	10.4 ± 0.1
Adriatic	0.22 ± 0.01	0.27 ± 0.01	-0.33 ± 0.01	-0.27 ± 0.01	-0.29 ± 0.01	0.32 ± 0.01	10.5 ± 0.2
Tyrrhenian	0.21 ± 0.01	0.26 ± 0.01	-0.32 ± 0.01	-0.26 ± 0.01	-0.28 ± 0.01	0.30 ± 0.01	10.8 ± 0.1
Western	0.21 ± 0.01	0.24 ± 0.01	-0.30 ± 0.01	-0.24 ± 0.01	-0.26 ± 0.01	0.28 ± 0.01	11.2 ± 0.1
Atlantic	0.18 ± 0.01	0.21 ± 0.01	-0.24 ± 0.02	-0.21 ± 0.01	-0.22 ± 0.01	0.23 ± 0.02	12.2 ± 0.5
DEEP	γ_{DIC}	β_{DIC}	ω_{DIC}	γ_{TA}	β_{TA}	ω_{TA}	Revelle
Aegean	0.22 ± 0.01	0.27 ± 0.01	-0.34 ± 0.01	-0.27 ± 0.01	-0.30 ± 0.01	0.32 ± 0.01	10.3 ± 0.1
Levantine	0.22 ± 0.01	0.27 ± 0.01	-0.34 ± 0.01	-0.27 ± 0.01	-0.29 ± 0.01	0.32 ± 0.01	10.4 ± 0.1
Ionian	0.22 ± 0.01	0.27 ± 0.01	-0.34 ± 0.01	-0.27 ± 0.01	-0.29 ± 0.01	0.32 ± 0.01	10.4 ± 0.1
Adriatic	0.22 ± 0.01	0.26 ± 0.01	-0.33 ± 0.01	-0.26 ± 0.01	-0.28 ± 0.01	0.31 ± 0.01	10.6 ± 0.1
Tyrrhenian	0.21 ± 0.01	0.25 ± 0.01	-0.31 ± 0.01	-0.25 ± 0.01	-0.27 ± 0.01	0.30 ± 0.01	10.9 ± 0.1
Western	0.21 ± 0.01	0.24 ± 0.01	-0.30 ± 0.01	-0.24 ± 0.01	-0.26 ± 0.01	0.29 ± 0.01	10.9 ± 0.1
Atlantic	0.17 ± 0.01	0.20 ± 0.01	-0.23 ± 0.01	-0.20 ± 0.01	-0.21 ± 0.01	0.22 ± 0.01	12.6 ± 0.3
BOTTOM	γ_{DIC}	β_{DIC}	ω_{DIC}	γ_{TA}	β_{TA}	ω_{TA}	Revelle
Aegean	–	–	–	–	–	–	–
Levantine	0.20 ± 0.01	0.24 ± 0.01	-0.30 ± 0.01	-0.24 ± 0.01	-0.26 ± 0.01	0.29 ± 0.01	9.4 ± 0.1
Ionian	0.22 ± 0.01	0.27 ± 0.01	-0.33 ± 0.01	-0.27 ± 0.01	-0.29 ± 0.01	0.32 ± 0.01	10.4 ± 0.1
Adriatic	–	–	–	–	–	–	–
Tyrrhenian	0.21 ± 0.01	0.25 ± 0.01	-0.31 ± 0.01	-0.25 ± 0.01	-0.27 ± 0.01	0.29 ± 0.01	11.0 ± 0.1
Western	0.21 ± 0.01	0.25 ± 0.01	-0.30 ± 0.01	-0.25 ± 0.01	-0.27 ± 0.01	0.29 ± 0.01	11.1 ± 0.1
Atlantic	–	–	–	–	–	–	–

$$\gamma_{\text{DIC}} = \text{DIC} - \frac{\text{TA}_C^2}{S}$$

$$\gamma_{\text{TA}} = \frac{\text{TA}_C^2 - \text{DIC} \times S}{\text{TA}_C}$$

$$\beta_{\text{DIC}} = \frac{\text{DIC} \times S - \text{TA}_C^2}{\text{TA}_C}$$

$$\beta_{\text{TA}} = \frac{\text{TA}_C^2}{\text{DIC}} - S$$

$$\omega_{\text{DIC}} = \text{DIC} - \frac{\text{TA}_C \times (2 \times [\text{CO}_2] + [\text{HCO}_3^-])}{P}$$

$$\omega_{\text{TA}} = \text{TA}_C - \frac{\text{DIC} \times P}{2 \times [\text{CO}_2] + [\text{HCO}_3^-]}$$

$$S = [\text{HCO}_3^-] + 4 \times [\text{CO}_3^{2-}] + \frac{[\text{H}^+] \times [\text{B}(\text{OH})_4^-]}{K_{hb} + [\text{H}^+]} + [\text{H}^+] + [\text{OH}^-]$$

$$P = [\text{HCO}_3^-] - \frac{[\text{H}^+] \times [\text{B}(\text{OH})_4^-]}{K_{hb} + [\text{H}^+]} - [\text{H}^+] - [\text{OH}^-]$$

$$\text{TA}_C = [\text{HCO}_3^-] + 2 \times [\text{CO}_3^{2-}]$$

$$\text{DIC} = [\text{HCO}_3^-] + [\text{CO}_3^{2-}] + [\text{CO}_2]$$

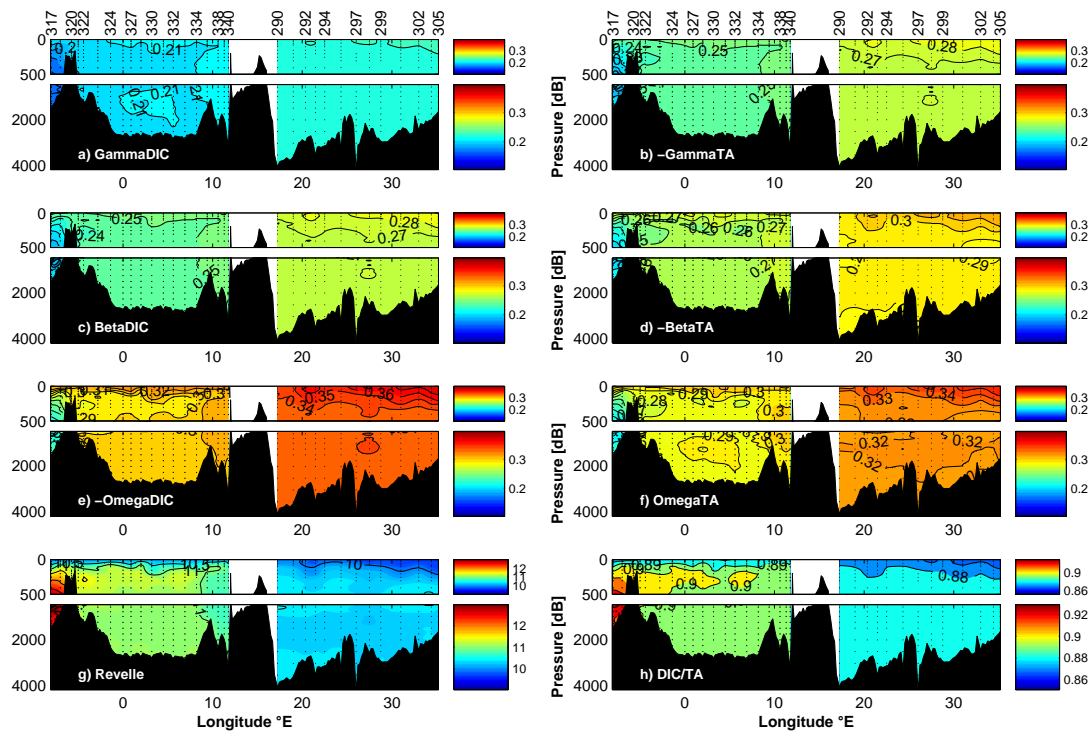


Fig. 10. Vertical distribution in the Mediterranean Sea from the Meteor cruise M84/3 of the buffer factors (a) γ_{DIC} , (b) $-\gamma_{TA}$, (c) β_{DIC} , (d) $-\beta_{TA}$, (e) $-\omega_{DIC}$, (f) ω_{TA} , all in mmol kg^{-1} , (g) Revelle factor and (h) DIC/TA ratio, both dimensionless.

- By examining the Revelle factor it is obvious that for a given change in CO₂ the relative change in DIC for MedSea waters is higher than in the adjacent Atlantic waters. That means that MedSea waters have the ability to store more anthropogenic carbon (C_{ANT}) than Atlantic waters. Within the MedSea the eastern basin is more prone to absorb more C_{ANT} for a given CO₂ increase than the western basin.

The impact of the three main anthropogenic processes altering the surface CO₂ chemistry in MedSea waters is given in Table 4, which shows absolute changes in aqueous CO₂ ([CO₂]), pH and the aragonite saturation (Ω -Ar) from the initial surface values in Table 2; the different sub-basins are treated separately. A C_{ANT} input through air-sea exchange (affecting DIC at constant TA) increasing DIC by $10 \mu\text{mol kg}^{-1}$ will lead to an increase of [CO₂] from 0.56 to $0.78 \mu\text{mol kg}^{-1}$, a pH decrease of around 0.016 units in MedSea waters, less than the pH decrease in Atlantic waters (0.020) for the same perturbation; the saturation state is reduced by about 0.1 units, but a reduction of at least 0.9 is required for deep waters to become under-saturated in aragonite. A hypothetical decrease in calcification, resulting in a DIC increase of $10 \mu\text{mol kg}^{-1}$ and double in TA, will compensate the pH and Ω decrease due to the input of C_{ANT} and roughly half the corresponding increase in [CO₂]. Within the MedSea changes in [CO₂] and pH increase westwards being

smaller than in Atlantic waters. An increase in salinity of 0.03 will cause minor changes in the CO₂ chemistry.

The buffer factors here provided are useful to predict changes in the CO₂ chemistry as a function of DIC and/or TA changes due to different processes, natural and/or anthropogenic. However, it is relevant to relate the increase of C_{ANT} in the ocean to the increasing partial pressure of CO₂ ($p\text{CO}_2$) in the atmosphere instead of using a DIC increase as reference. Table 5 shows the absolute changes in DIC, pH and Ω -Ar from initial states in Table 2 as a consequence of prescribed $p\text{CO}_2$ increases. Note that a $p\text{CO}_2$ increase of $25 \mu\text{atm}$ causes changes in DIC by about $10 \mu\text{mol kg}^{-1}$, as already presented in Table 4. The main result in Table 5 is that as the Revelle factor in warm, salty and high TA waters is lower and the other buffer factors distribute as $|\omega| > |\beta| > \gamma_{DIC}$ (Table 3), the change in DIC and Ω -Ar for a given $p\text{CO}_2$ increase is higher in the MedSea, but that for pH is lower than in the Atlantic. Therefore, MedSea waters are more (less) sensitive to DIC and Ω -Ar (pH) changes induced from the $p\text{CO}_2$ increase in the atmosphere (C_{ANT} increase).

4.2 Water mass characterisation

Here we present property-property plots for general physical and chemical variables, typical potential temperature-salinity, AOU-salinity and silicate concentration (SiO₂)-salinity (Figs. 11 and 13) and the CO₂ variables, TA, DIC and

Table 4. Absolute associated changes in aqueous [CO₂] (μmol kg⁻¹), pH (no units) and aragonite saturation (no units) state due to several processes related to global change: a DIC increase of 10 μmol kg⁻¹ at constant TA (CO₂ air-sea exchange), a decrease in calcification of 10 μmol kg⁻¹ in DIC and double in TA, a salinity increase of 0.03. Surface values from Table 2 and 3 are taken to perform the calculations.

Air-sea CO ₂ gas exchange ΔDIC = + 10 μmol kg ⁻¹			
	Δ[CO ₂]	ΔpH	ΔOmega
Aegean	0.56	-0.016	-0.10
Levantine	0.57	-0.016	-0.10
Ionian	0.62	-0.017	-0.07
Adriatic	0.62	-0.016	-0.10
Tyrrhenian	0.77	-0.018	-0.10
Western	0.76	-0.018	-0.10
Atlantic	0.78	-0.020	-0.10
Calcification decrease ΔDIC = +10 μmol kg ⁻¹ ΔTA = +20 μmol kg ⁻¹			
	Δ[CO ₂]	ΔpH	ΔOmega
Aegean	-0.36	0.011	0.11
Levantine	-0.36	0.011	0.11
Ionian	-0.40	0.012	0.11
Adriatic	-0.40	0.012	0.11
Tyrrhenian	-0.52	0.013	0.11
Western	-0.52	0.013	0.11
Atlantic	-0.53	0.015	0.11
Salinity increase			
	Δ[CO ₂]	ΔpH	ΔOmega
Aegean	0.01	0.0001	0.004
Levantine	0.01	0.0001	0.004
Ionian	0.01	0.0001	0.002
Adriatic	0.01	0.0001	0.004
Tyrrhenian	0.01	0.0001	0.003
Western	0.01	0.0001	0.003
Atlantic	0.01	0.0001	0.003

pH_{25T} vs. salinity, SiO₂ and AOU (Figs. 12 and 14). We separated the western and eastern basins showing with colours the different sub-basins comprised. Some special characteristics, mainly in deep waters, are presented in more detail with figures in the Supplement. The companion paper by Hainbucher et al. (2013) gives more details about the physical and hydrodynamical variability.

4.2.1 Aegean Sea (stations 287, 288 and 289)

Three stations during the M84/3 cruise were located in the Aegean Sea: 287 in the Chios Basin (central Aegean Sea), 289 in the eastern Cretan basin and 289 in the Kasos Strait

Table 5. Absolute associated changes in DIC concentration, pH and aragonite saturation state due several partial pressure of CO₂ in the atmosphere increase. The initial conditions are the mean 2011 values (Table 2).

	ΔDIC in μmol kg ⁻¹			
	25 μatm	100 μatm	200 μatm	300 μatm
Aegean	13.1	52.4	104.8	157.2
Levantine	13.0	52.1	104.2	156.3
Ionian	12.9	51.6	103.1	154.7
Adriatic	11.9	47.8	95.5	143.3
Tyrrhenian	9.7	38.8	77.7	116.5
Western	9.8	39.1	78.2	117.2
Atlantic	10.8	43.3	86.6	129.9
	ΔΩ – Ar			
	25 μatm	100 μatm	200 μatm	300 μatm
Aegean	-0.13	-0.52	-1.05	-1.57
Levantine	-0.13	-0.52	-1.04	-1.56
Ionian	-0.13	-0.52	-1.03	-1.55
Adriatic	-0.12	-0.48	-0.96	-1.43
Tyrrhenian	-0.10	-0.38	-0.76	-1.14
Western	-0.10	-0.38	-0.77	-1.15
Atlantic	-0.11	-0.43	-0.85	-1.28
	ΔpH			
	25 μatm	100 μatm	200 μatm	300 μatm
Aegean	-0.020	-0.088	-0.199	-0.349
Levantine	-0.021	-0.089	-0.200	-0.350
Ionian	-0.022	-0.094	-0.215	-0.383
Adriatic	-0.019	-0.083	-0.186	-0.321
Tyrrhenian	-0.017	-0.073	-0.160	-0.269
Western	-0.017	-0.074	-0.164	-0.278
Atlantic	-0.022	-0.095	-0.216	-0.384

(both in the southern Aegean Sea). In the upper 100 dbars high salinity identifies LSW (Levantine Surface Water) entering the Aegean Sea through the eastern Cretan arc straits (Fig. 11a). This LSW was also identified by the highest pH_{25T} values measured in the M84/3 cruise (> 8.01, Fig. 12h) and also high TA and DIC values (≈ 2620 and ≈ 2280 μmol kg⁻¹, respectively, Fig. 12a and d). At intermediate levels, 100 to 250 dbars, CIW (Cretan Intermediate Water) presented the highest TA values for the M84/3 cruise (≈ 2645 μmol kg⁻¹, Fig. 12a and d). Deep layers below 2500 dbars were occupied by CDW (Cretan Deep Water), warm, salty and very dense (Fig. 11a), also identified by the distinct SiO₂-salinity relation (Fig. 11c), practically constant DIC (≈ 2320 μmol kg⁻¹) and TA (≈ 2630 μmol kg⁻¹) values vs. SiO₂ (Fig. 12b and e).

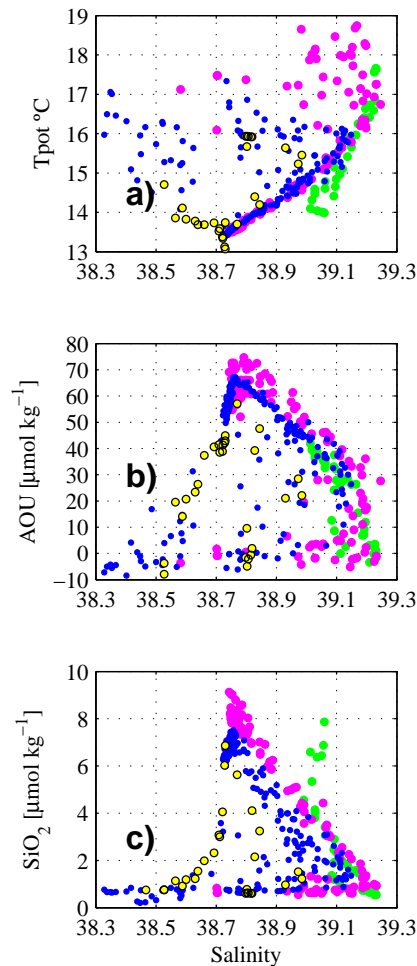


Fig. 11. Property-property plots for the M84/3 data in the eastern basin: Aegean Sea (green dots), Levantine basin (magenta), Ionian Sea (blue) and Adriatic Sea (yellow). (a) Potential temperature (°C) vs. salinity, (b) Apparent Oxygen Utilisation (AOU in $\mu\text{mol kg}^{-1}$) vs. salinity and (c) silicate concentration (SiO_2 in $\mu\text{mol kg}^{-1}$) vs. salinity. The station positions are shown in Fig. 1.

4.2.2 Levantine Basin (from station 290 to 298)

In the upper water column, < 100 dbars, AW and LSW could be distinguished using salinity (Fig. 11a), LSW presented salinity > 38.9 and AW from 38.58 to 38.9 (Fig. 11a). TA, DIC and pH25T values much higher in LSW could also differentiate them (Fig. 12a, d and g). Interestingly, LSW presented pH25T values higher, and AW lower than 8.01 for waters with AOU < 0 (Fig. 12i).

At intermediate depths, 100–400 dbars, the main water mass was LIW (Levantine Intermediate Water). In addition to the typical scorpion tail relation between salinity and potential temperature, LIW was recognized by SiO_2 minima associated with a salinity maximum (Fig. 11c) and high TA ($\approx 2630 \mu\text{mol kg}^{-1}$, Fig. 12a) values.

In the deep layers below 1000 dbars within the Levantine basin, the salinity minimum and then a pronounced temperature-salinity inversion (temperature and salinity increase) typically detected during the EMT (Roether et al., 2007) was still detected in this basin (Hainbucher et al., 2013) (red lines in Fig. S1). Water in the inversion is EMDW with an Aegean Sea origin (Aeg-EMDW) produced during the EMT.

Adriatic EMDW (Ad-EMDW) to the west of the East Mediterranean Ridge was differentiated from Aeg-EMDW mainly with AOU and SiO_2 (Fig. 11b and c), both being lower in the Ad-EMDW, which also contained higher transient tracer values (Stöven and Tanhua, 2013), indicating a more recent origin. It is difficult to separate them using TA, DIC and pH25T, both EMDW presented similar values, Ad-EMDW was slightly higher in DIC (around $5 \mu\text{mol kg}^{-1}$) and TA (around $4 \mu\text{mol kg}^{-1}$) and lower in pH25T (0.005 pH units) than Aeg-EMDW (Fig. 12c, f and i) (blue and black lines in Fig. S1).

The salinity minimum around 1000 dbars and below the temperature-salinity inversion previously commented provoke a sort of hook in the relationship between DIC – TA – pH25T vs. AOU or SiO_2 (red lines in Fig. S1) for deep waters in this basin. DIC and TA decrease with decreasing SiO_2 or AOU until their corresponding maxima (salinity minimum) and then towards the bottom DIC and TA increase with decreasing AOU (increasing salinity). pH is the opposite, it decreases with AOU increasing until the AOU maximum (salinity minimum) and then pH increases and AOU decreases (Fig. S1).

4.2.3 Ionian Sea (from station 299 to 309, 314 and 315)

Two upper water masses could be differentiated in the Ionian Sea, AW (< 17 °C, < 38.9) and LSW (> 16 °C, > 38.8) (Fig. 11a). During M84/3 LSW in the Ionian Sea was found in the stations to the western part of the Hellenic Trench (Sts. 299, 300, 301) (Fig. 1). Below, two intermediate water masses, LIW and CIW could be distinguished. LIW with temperature and salinity maxima around 200 dbars was also associated with a TA and DIC maximum (Fig. 12a and d). The mixing between LIW and AW produced an exponential relationship between TA and DIC vs. salinity (Fig. 12a and d). Deviations from this relationship towards lower TA and DIC values corresponded to LSW in this basin. The other intermediate water detected, CIW, mixed with LIW south of Crete, in the eastern basin was found in stations 299, 300 and 301 to the west of the Antikithera strait. This water mass with also very high salinity, presented an even higher TA than LIW (Fig. 12a, b and c). For example in the case of the TA vs. SiO_2 plot (Fig. 12b) CIW was detected as a deviation towards higher values from the typical TA – SiO_2 relationship. CIW was also seen as a hump between 0 to $30 \mu\text{mol kg}^{-1}$ AOU over the LIW data (Fig. 12c).

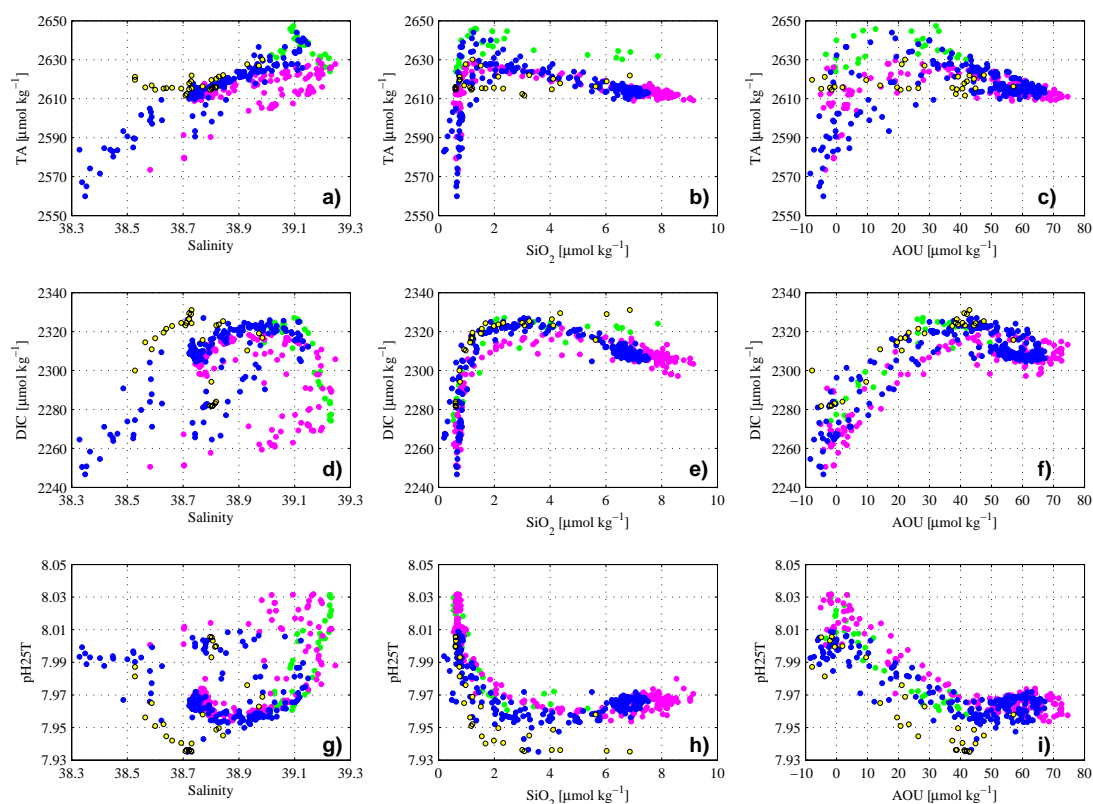


Fig. 12. Property-property plots for the M84/3 data in the eastern basin: Aegean Sea (green dots), Levantine basin (magenta), Ionian Sea (blue) and Adriatic Sea (yellow). First row: alkalinity (TA in $\mu\text{mol kg}^{-1}$) vs. (a) salinity, (b) silicate concentration (SiO_2 in $\mu\text{mol kg}^{-1}$) and (c) AOU ($\mu\text{mol kg}^{-1}$). Second row: Dissolved Inorganic Carbon (DIC in $\mu\text{mol kg}^{-1}$) vs. (d) salinity, (e) SiO_2 and (f) AOU. Third row: pH25T vs. (d) salinity, (e) SiO_2 and (f) AOU. The station positions are shown in Fig. 1.

In the Ionian Sea, Post-EMT-EMDW occupied the layer below 1500 dbars, it presented lower AOU and SiO_2 values than EMT Aeg-EMDW (Fig. 11b and c) in the Levantine basin. The recent replenishment from the Adriatic Sea, 2001 onwards, was detected as a temperature-salinity increase in bottom waters of the central Ionian Sea (Rubino and Hainbucher, 2007) (green and cyan lines in Fig. S2). These younger bottom waters in the Ionian Sea explain the DIC increase (Fig. 6), AOU and pH25T (Fig. 7) decrease towards the bottom of the Ionian Sea (compare red line with the blue and cyan lines in Fig. S2).

The hook structure in the relationships DIC – TA – pH vs. AOU for deep waters in the Levantine basin (Fig. S1) was here eroded as is the temperature-salinity inversion associated with EMT Aeg-EMDW. The AOU maximum in the Ionian Sea was no longer as clearly associated with the salinity minimum as in the Levantine basin. Below 500 dbars DIC and TA decrease with increasing AOU, from the AOU maximum TA practically stays constant and DIC increases. The very recent input of bottom Ad-EMDW is noticed in the pH vs. AOU relationship, from 500 dbars pH decreases with AOU increasing, from the AOU maximum pH increases

(AOU decreases) but close to the bottom both pH and AOU decrease (Fig. S2).

4.2.4 Adriatic Sea (stations 310 and 313)

Only two stations were sampled in the Adriatic Sea for CO₂ variables, one in the Adriatic Pit (313) and one to the east of the Otranto Strait (310). One of the densest deep waters during the M84/3 cruise was sampled in the Adriatic Pit at 1100 dbars (Fig. 11a), this water remains confined as the Otranto Strait is only 800 m deep. Waters in the Adriatic presented high TA values despite a moderate salinity (Fig. 12a), they were out of the general linear relationship between TA and salinity due to the high TA of the rivers discharging in the area (Luchetta et al., 2010; Cantoni et al., 2012; Copin-Montegut, 1993). The relationship TA vs. SiO_2 was also different for Adriatic waters (Fig. 12b), being lower than the general trend in the eastern MedSea. Additionally DIC and pH in the Adriatic had a distinct signal, high values for DIC and low values for pH in waters with salinity lower than 38.7 (Fig. 12d and g).

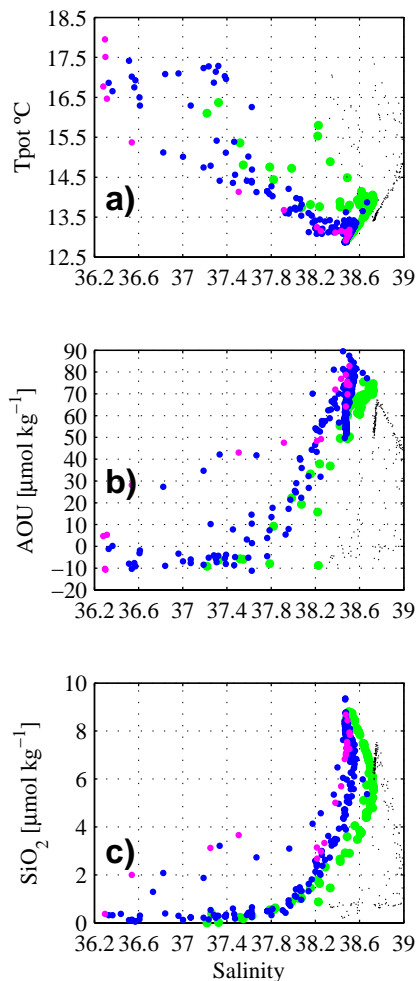


Fig. 13. Property-property plots for the M84/3 data in the western basin: Tyrrhenian Sea (green dots), Western basin (blue) and Strait of Gibraltar (magenta). Light black dots correspond to Ionian Sea data. (a) Potential temperature (°C) vs. salinity and (b) Apparent Oxygen Utilisation (AOU in $\mu\text{mol kg}^{-1}$) vs. salinity and (c) silicate concentration (SiO_2 in $\mu\text{mol kg}^{-1}$) vs. salinity. The station positions are shown in Fig. 1.

The current overflow from the Adriatic stood out in the pH – AOU plot (Figs. 14i and 7, upper panel): pH data for AOU values between 40 and 45 $\mu\text{mol kg}^{-1}$ in stations 309 and 310 located in the Otranto Strait, deviated towards 7.94 pH25T values, corresponding to waters around 500 dbars in the Adriatic Pit.

4.2.5 Tyrrhenian Sea (from station 316 to 321)

This basin acts as a connector between the eastern and the western MedSea, here intermediate waters entering from the east mix with deep waters entering from the west (e.g. Hopkins, 1988; Astraldi et al., 1996). This fact was noticed in the property-property plots shown in Fig. 13 were the points

corresponding to the Tyrrhenian Sea clearly connected the western and eastern MedSea waters.

In the surface layer, AW with salinity lower than 38 was detected in all the Tyrrhenian stations except 319 in the centre of the basin (Fig. 13a). The freshest AW was seen in station 316, the nearest to Sicily, here AW comes directly from Gibraltar through the Algerian sub-basin. AW was also distinguished by low AOU and SiO_2 values close to zero (Fig. 13b and c). The minimum TA and DIC associated with AW are 2466 and 2178 $\mu\text{mol kg}^{-1}$, respectively (Fig. 14a and d). In the centre of the Tyrrhenian Sea the upper 52 dbars were occupied by probably modified AW with $38.5 > \text{salinity} > 38$ affected by evaporation or mixed with the salty intermediate water entering through the Strait of Sicily. This water also presented a different relationship between salinity and pH25T compared to unmixed AW (Fig. 14g).

Maximum salinity values in the intermediate layer between 250 and 500 dbars pointed to LIW entering from the eastern basin (Fig. 13a). As LIW flows into the Tyrrhenian Sea remineralization processes increase its AOU, DIC and lower pH25T, with extreme values found in St. 319 (cyan line in Fig. S3) in the interior of this basin and at St. 321 (magenta line in Fig. S3) in the Sardinia Channel where aged LIW flows out of the Tyrrhenian Sea into the western basin.

At St. 316 (red line in Fig. S3), the nearest one to Sicily in the Sardinia Sicily passage, the intermediate layer was occupied by a fresher LIW (38.66–38.68) with higher AOU and DIC (lower pH25T and TA) values. It might be LIW mixed with AW returning to the western basin although this is an area where LIW is supposed to enter the Tyrrhenian Sea.

Deep layers in the Tyrrhenian are occupied by TDW with a typical linear relationship in the temperature-salinity plot (Fig. 13a). No hook in the temperature-salinity diagram to lower salinities was detected in bottom waters of the Tyrrhenian Sea, this hook would show the input of recently formed WMDW as detected in the bottom of the western basin. In the Tyrrhenian Sea bottom WMDW stands out from TDW by the sharp decrease in AOU and pH25T (Fig. 7) and increase in DIC (Fig. 6) for example with salinity (red dots in Fig. S4).

4.2.6 Western basin (from station 322 to 336)

The upper layer in this basin was occupied by AW very fresh ($\ll 38$) and practically 100 % saturated in oxygen ($\text{AOU} \approx 0 \mu\text{mol kg}^{-1}$) and with no SiO_2 (Fig. 13b and c). In the intermediate layer the salinity maximum associated with LIW evolves from 38.67 at St. 322 to 38.51 at St. 336. There was a marked reduction in salinity (and TA) when LIW entered the western basin passing from 38.71 at St. 321 in the Sardinia Channel, 38.67 at St. 322 (right west of the channel) and then 38.51 at St. 323 in the western basin. The change in the other chemical variables, SiO_2 , AOU, DIC or pH25T was less acute.

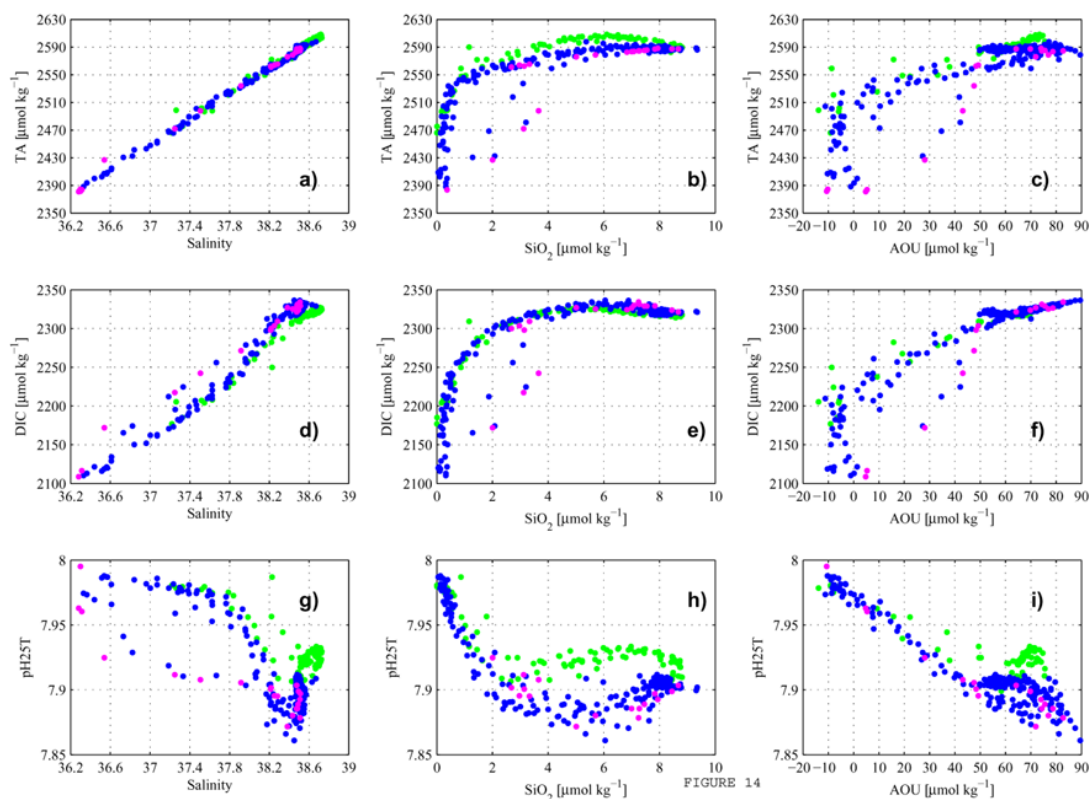


Fig. 14. Property-property plots for the M84/3 data in the western basin: Tyrrhenian Sea (green dots), Western basin (blue) and Strait of Gibraltar (magenta). First row: alkalinity (TA in $\mu\text{mol kg}^{-1}$) vs. (a) salinity, (b) silicate concentration (SiO_2 in $\mu\text{mol kg}^{-1}$) and (c) AOU ($\mu\text{mol kg}^{-1}$). Second row: Dissolved Inorganic Carbon (DIC in $\mu\text{mol kg}^{-1}$) vs. (d) salinity, (e) SiO_2 and (f) AOU. Third row: pH25T vs. (d) salinity, (e) SiO_2 and (f) AOU. The station positions are shown in Fig. 1.

When in the western basin, LIW was associated with a maximum in AOU (Fig. 13b), DIC (Fig. 14d) and minimum in pH25T (Fig. 14g), so it was the layer of maximum remineralization of organic matter, contrary to the eastern basin where this layer was right below LIW.

The near bottom layer in the western basin was occupied by a recently formed WMDW with higher salinity, so the temperature-salinity plots present a sort of hook structure (Hainbucher et al., 2013). This new WMDW presented higher DIC and lower AOU than the older WMDW (Figs. 14f and S5).

4.2.7 Atlantic waters (from station 337 to 344)

Due to the dramatic scale change, Figs. 13 and 14 show only the data up to St. 338 (corresponding to the Strait of Gibraltar). All the samples collected to the west of this Strait are shown in Fig. S6.

At the Strait of Gibraltar (St. 337 and 338) the intermediate LIW outflowing presented a salinity of 38.48 ($\text{TA} \approx 2584 \mu\text{mol kg}^{-1}$, $\text{DIC} \approx 2331 \mu\text{mol kg}^{-1}$, $\text{pH}_{25\text{T}} \approx 7.89$, $\text{AOU} \approx 75.3 \mu\text{mol kg}^{-1}$) (Figs. 14 and S6). The outflow was only detected at stations

342 and 344 (pink lines in Fig. S6) in the Portuguese continental slope, with a salinity of 36.50 ($\text{TA} \approx 2409 \mu\text{mol kg}^{-1}$, $\text{DIC} \approx 2193 \mu\text{mol kg}^{-1}$, $\text{pH}_{25\text{T}} \approx 7.86$, $\text{AOU} \approx 58.2 \mu\text{mol kg}^{-1}$). In the centre of the Gulf of Cádiz (339 and 340, black and green lines respectively in Fig. S6), the outflow was mixed with the upper low salinity central waters and presented a salinity of 36.20 ($\text{TA} \approx 2392 \mu\text{mol kg}^{-1}$, $\text{DIC} \approx 2202 \mu\text{mol kg}^{-1}$, $\text{pH}_{25\text{T}} \approx 7.79$, $\text{AOU} \approx 93 \mu\text{mol kg}^{-1}$).

5 Summary

Two coordinated cruises sampled the Mediterranean Sea for CO₂ variables (TA, DIC and pH) in 2011: the RV Urania EF11 (Sardinia Sicily passage) and the RV Meteor M84/3 (East-West full-length transect).

The over-determined and high-quality CO₂ data collected in the M84/3 cruise allowed performing the first internal consistency analysis for CO₂ data in the peculiar warm, salty and low DIC/TA ratio MedSea waters. Using the [®]MATLAB version for the consensus CO2SYS programme the preferred set of constants is option 4 [CO₂ constants from Mehrbach

et al. (1973) refitted by Dickson and Millero (1987)] along with the sulphate constant from Dickson (1990) and the parameterization of borate from Uppström (1974). Using this combination our pH, TA and DIC measurements from the M84/3 cruise are internally consistent to -0.0003 ± 0.005 for pH, $0.1 \pm 3.3 \mu\text{mol kg}^{-1}$ for TA and $-0.1 \pm 3 \mu\text{mol kg}^{-1}$ for DIC. Despite this encouraging result further studies are needed including a fourth variable: $p\text{CO}_2$ in order to verify the internal consistency of K_1 (only a reliable K_1 is needed to calculate $p\text{CO}_2$ from the input of pH – TA or pH – DIC) and $[\text{CO}_3^{2-}]$ in order to revise the K_2 parameterization in low DIC/TA ratio waters where the CO₂ system is more sensitive to K_2 . Using the combination of pH – TA – DIC only a reliable K_2 is needed in order to calculate bicarbonate, carbonate and aqueous CO₂ (Park, 1969). Particularly comparing measured (Byrne and Yao, 2008) and calculated $[\text{CO}_3^{2-}]$ could be helpful to revise K_2 .

The Meteor M84/3 data allowed a post-EMT, full length and depth description of CO₂ variables in the MedSea. This study aims to be base-line for future data and model studies dealing with the effects of natural (climate) and human (warming, acidification, etc. . .) driven changes in the CO₂ species and ancillary variables associated.

As a general view, the eastern MedSea presents higher TA ($2560\text{--}2644 \mu\text{mol kg}^{-1}$) and pH25T (7.935–8.032) and less variable DIC ($2247\text{--}2331 \mu\text{mol kg}^{-1}$) than the western basin with TA ($2388\text{--}2608 \mu\text{mol kg}^{-1}$), pH25T (7.861–7.988) and DIC ($2110\text{--}2336 \mu\text{mol kg}^{-1}$). The saturation for calcite and aragonite in both basins is well above 1, for the eastern basin $\Omega\text{-Ca}$ vary 2.5–5.78 and $\Omega\text{-Ar}$ 1.73–3.80 and for the western basin $\Omega\text{-Ca}$ 2.73–5.25 and $\Omega\text{-Ar}$ 1.86–3.44.

The CO₂ chemistry in the warm, salty and high TA waters in the MedSea compared to the Atlantic is in general less sensitive to temperature changes because of the low DIC/TA ratio. MedSea waters are more resistant to direct changes in DIC and/or TA due to natural and/or anthropogenic processes, since the calculated buffer factors are higher in MedSea waters, showing an increasing westwards gradient. The CO₂ chemistry in the western basin would be more sensitive than in the eastern basin.

However, from the point of view of an increasing $p\text{CO}_2$ in the atmosphere, that increases indirectly DIC and keeps TA constant in the ocean, waters in the MedSea have a lower Revelle factor than in the Atlantic, and therefore are able to store more DIC for a given $p\text{CO}_2$ increase than in the Atlantic but the changes in pH (Ω) would be lower (higher) than in the Atlantic.

As a summary the water masses encountered according to depth are:

- i. Levantine Surface Water (LSW): warm and salty (> 38.9) surface water (upper 100 dbars) formed by intensive heating and evaporation in the Levantine basin, found during the M84/3 cruise in this basin and the Aegean and Ionian Seas. LSW was

characterised by high TA ($\approx 2610 \mu\text{mol kg}^{-1}$) and DIC ($\approx 2270 \mu\text{mol kg}^{-1}$). In April 2011 LSW presented pH25T > 8.01 associated with AOU < 0 pointing to active photosynthetic activity.

- ii. Atlantic Water (AW): it is the upper part (< 125 dbars) of the open estuarine cell in the MedSea, enters through the Strait of Gibraltar and flows to the Levantine basin while suffering evaporation and heating. The main CO₂ variable showing the presence of AW is TA, which evolved from very low values in the Strait of Gibraltar ($\approx 2390 \mu\text{mol kg}^{-1}$) to high values ($\approx 2610 \mu\text{mol kg}^{-1}$) in the Levantine basin. Evaporation processes and mixing with the salty Levantine Intermediate Water (LIW) induced a practically linear relation between TA and salinity. Another linear relationship was found between pH25T and AOU for the western MedSea in April 2011 pointing to a biological modulation of pH.
- iii. Levantine Intermediate Water (LIW): main intermediate water mass in the MedSea (125–500 dbars), is the lower part of the open estuarine cell in the MedSea. Typically LIW is identified by a scorpion tail in the temperature-salinity diagram associated with a salinity maximum. The main CO₂ variable identifying LIW in any MedSea sub-basin was an intermediate TA maximum evolving from $\approx 2620 \mu\text{mol kg}^{-1}$ in the Levantine and Ionian basins to $\approx 2600 \mu\text{mol kg}^{-1}$ in the Tyrrhenian Sea, $\approx 2590 \mu\text{mol kg}^{-1}$ in the western basin, and $\approx 2584 \mu\text{mol kg}^{-1}$ overflowing in the Strait of Gibraltar, and finally $\approx 2409 \mu\text{mol kg}^{-1}$ in the Mediterranean Water located in the Gulf of Cadiz, that then circulates into the North Atlantic.
In the Levantine and Ionian basins LIW was found shallower (≈ 250 dbars) than in the western basin (≈ 450 dbars). In the eastern MedSea LIW was situated above the layer of maximum organic matter mineralization while in the western MedSea they coincided and therefore was associated with a maximum in DIC and AOU and minimum in pH.
- iv. Cretan Intermediate Water (CIW): formed in the Cretan Sea, this intermediate (250 dbars) water was characterised by even higher TA ($2630\text{--}2645 \mu\text{mol kg}^{-1}$) than LIW and detected in the Aegean Sea and the Ionian Sea west of the Antikithera strait.
- v. Cretan Deep Water (CDW): produced by convection in the Cretan Sea, was clearly identified apart of the high density, by a distinct relation between SiO₂ – salinity, high constant TA ($2630 \mu\text{mol kg}^{-1}$) and DIC ($2320 \mu\text{mol kg}^{-1}$) values with varying SiO₂ ($2\text{--}4 \mu\text{mol kg}^{-1}$). This water remained confined in the Aegean Sea.

- vi. Pre-EMT Eastern Mediterranean Deep Water (EMDW): this water mass, of an Adriatic Sea origin, was still detected in the Levantine basin by a salinity minimum around 1000 dbars, it presented a minimum in tracer values as CFC-12 or SF₆, but also a minimum in pH because was the layer of organic matter remineralization as also indicated by the maximum in AOU and inorganic nutrients.
- vii. EMT-EMDW: below the salinity minimum in the Levantine basin temperature and salinity increase producing a hook in the temperature-salinity diagram which is associated with the input of EMDW produced in the Aegean Sea during the EMT. Due to a more recent origin it presents lower AOU, slightly higher DIC and pH values than pre-EMT EMDW.
- viii. Post-EMT-EMDW: bottom layers in the Hellenic Trench (Levantine basin) and deep layers (> 1000 dbars) in the Ionian Sea are occupied by EMDW with an Adriatic origin produced after the EMT. The hook in the temperature-salinity diagram was no longer detected and a less salty post-EMT-EMDW occupied the deep layer in the Ionian Sea. This water was also identified by lower AOU and pH values compared to the saltier EMT-EMDW.
- Bottom layers in the Ionian Sea, below about 3000 dbars, were occupied by recent overflow waters produced in the Adriatic Sea after 2001. It presented a clear signature in DIC (> 2310 $\mu\text{mol kg}^{-1}$), AOU (< 55 $\mu\text{mol kg}^{-1}$) and pH (< 7.967).
- ix. Waters in the Adriatic Sea: surface waters in this basin presented a distinct TA vs. salinity relationship with values around 2610 $\mu\text{mol kg}^{-1}$ for salinity < 38.7, higher than the general TA-salinity relation mainly due to the high TA input through Adriatic rivers. The overflow from the Adriatic Sea was mainly detected in the pH vs. AOU relationship, for AOU values between 40–45 $\mu\text{mol kg}^{-1}$ pH deviated to 7.94, those are waters from around 500 dbars in the Adriatic Pit spilling into the Ionian Sea.
- x. Waters in the Tyrrhenian Sea: the property-property plots showed that this basin is a connector between the eastern and western basins, where LIW mixes with deep waters from the west producing Tyrrhenian Deep Water (TDW). During 2011 no recently formed Western Mediterranean Deep Water (WMDW) was detected in the bottom of the Tyrrhenian Sea.
- The water mass exchange between the eastern and western MedSea is highlighted using data from the Urania EF11 cruise in the Sardinia Sicily passage: AW mainly enters the Tyrrhenian on the eastern part of the passage, close to Sicily, and exits this basin on the Sardinian side, becoming saltier and also higher in TA;

the same circulation scheme is done by LIW, which becomes colder and saltier after circulating in the Tyrrhenian, TA is decreased and DIC increased.

- xi. Western Mediterranean Deep Water (WMDW): this water occupied layers below 1000 dbars in the western basin of the MedSea, with respect to CO₂ variables it presented DIC (2318–2320 $\mu\text{mol kg}^{-1}$) higher and TA (2584–2588 $\mu\text{mol kg}^{-1}$) and pH_{25T} (7.90–7.91) lower than EMDW. In the bottom layer a recent input, after 2005, of WMDW was detected with higher salinity and temperature, while DIC (AOU) clearly increased (decreased) towards the bottom.
- xii. In the Strait of Gibraltar LIW presented in 2011 a salinity of 38.48 and TA \approx 2584 $\mu\text{mol kg}^{-1}$, DIC \approx 2331 $\mu\text{mol kg}^{-1}$, pH_{25T} \approx 7.89, AOU \approx 75.3 $\mu\text{mol kg}^{-1}$; once mixed with central waters in the Gulf of Cadiz, Mediterranean Water sampled in the Portuguese slope was detected with a salinity of 36.50, TA \approx 2409 $\mu\text{mol kg}^{-1}$, DIC \approx 2193 $\mu\text{mol kg}^{-1}$, pH_{25T} \approx 7.86, AOU \approx 58.2 $\mu\text{mol kg}^{-1}$.

The CO₂ and ancillary data collected in 2011 highlight the need for a sustained programme monitoring the temporal evolution of water masses in the MedSea. This small but relevant marginal sea is a perfect laboratory basin to detect the effect of natural and anthropogenic driven changes in the physics and CO₂ chemistry. Special emphasis should be given to CO₂ variables as MedSea waters are especially sensitive to *p*CO₂ increases in the atmosphere: they are prone to absorb more DIC for given *p*CO₂ increase, this DIC increase in the surface is rapidly transported to depth with the overturning circulation, and therefore pH and carbonate saturation conditions are altered, with consequences still unknown for the well adapted organisms.

Acknowledgements. The authors want to thank the captains and crews on the research vessels R/V Meteor and R/V Urania for the excellent cooperation during the campaigns. The Meteor cruise M84/3 was supported by a grant from the Deutsche Forschungsgemeinschaft- Senatskommission für Ozeanographie (DFG), and from a grant from the DFG; TA 317/3-1. The participation of G. C. was partly supported by the Mediterranean Science Commission (CIESM). The authors are grateful to C. Colmenero-Modrón, I. Hueso-Zabaleta, F. Rozada and I. Buns for the technical assistance during CO₂, oxygen and inorganic nutrients sampling and analysis. Our special thanks to X. A. Álvarez-Salgado for providing some equipment. Funding for CO₂ measurements was provided by MICINN (MedSea Repeat, CTM2010-12244-E). This is a HOTMIX (CTM2011-30010-C02) contribution.

Edited by: M. Hoppema

References

- Álvarez, M.: The CO₂ system observations in the Mediterranean Sea: past, present and future, in: CIESM, Designing Med-SHIP: a Program for repeated oceanographic surveys, N° 43 in CIESM Workshop monographs, edited by: Briand, F., 164 pp., Monaco, 2012.
- Astraldi, M., Gasparini, G. P., Sparnocchia, S., Moretti, S., and Sansone, E.: The characteristics of the Mediterranean water masses and the water transport in the Sicily Channel at longtime scales, in: Dynamics of Straits and Channels, edited by: Briand, F., vol. 2, CIESM Science Series, Monaco, 95–118, 1996.
- Astraldi, M., Gasparini, G. P., Vetrano, A., and Vignudelli, S.: Hydrographic characteristics and interannual variability of water masses in the central Mediterranean: a sensitivity test for long-term changes in the Mediterranean Sea, *Deep Sea Res. I*, 49, 661–680, 2002.
- Azov, I.: The Mediterranean Sea, a marine desert?, *Mar. Pollut. Bull.*, 23, 225–232, 1991.
- Benson, B. B. and Krause Jr, D.: The concentration and isotopic fractionation of oxygen dissolved in freshwater and seawater in equilibrium with the atmosphere, *Limnol. Oceanogr.*, 29, 620–632, 1984.
- Bergamasco, A. and Malanotte-Rizzoli, P.: The circulation of the Mediterranean Sea: a historical review of experimental investigations, *Adv. Oceanogr. Limnol.*, 1, 11–28, doi:10.1080/19475721.2010.491656, 2010.
- Bosc, E., Bricaud, A., and Antoine, D.: Seasonal and interannual variability in algal biomass and primary production in the Mediterranean Sea, as derived from 4 years of SeaWiFS observations, *Global Biogeochem. Cy.*, 18, GB1005, doi:10.1029/2003GB002034, 2004.
- Brunet, C., Poisson, A., Lebel, J., and Porot, V.: Alcalinité totale, carbone inorganique, calcium, densité, in: Propriétés Hydrologiques et Chimiques des Eaux du Bassin Occidental de la Méditerranée. Campagne Mediproduct IV-15 Octobre–17 Novembre 1981, Résultats des Campagnes à la Mer, 26, 89–93, Centre National pour l'Exploitation des Océans, Brest, France, 1984.
- Byrne, R. H. and Yao, W. S.: Procedures for measurement of carbonate ion concentrations in seawater by direct spectrophotometric observations of Pb(II) complexation, *Mar. Chem.*, 112, 128–135, 2008.
- Cai, W.-J. and Wang, Y.: The chemistry, fluxes and sources of carbon dioxide in the estuarine waters of the Satilla and Altamaha Rivers, Georgia, *Limnol. Oceanogr.*, 43, 657–668, 1998.
- Cantoni, C., Luchetta, A., Celio, M., Cozzi, S., Raicich, F., and Catalano, G.: Carbonate system variability in the Gulf of Trieste (North Adriatic Sea), *Estuarine, Coast. Shelf Sci.*, 115, 51–62, doi:10.1016/j.eccs.2012.07.006, 2012.
- Claustre, H., Morel, A., Hooker, S. B., Babin, M., Antoine, D., Oubelkheir, K., Bricaud, A., Leblanc, K., Quéguiner, B., and Maritorena, S.: Is desert dust making oligotrophic waters greener?, *Geophys. Res. Lett.*, 29, doi:10.1029/2001GL014056, 2001.
- Clayton, T. D. and Byrne, R. H.: Spectrophotometric seawater pH measurements: total hydrogen ion concentration scale concentration scale calibration of m-cresol purple and at-sea results, *Deep-Sea Res. Pt. I*, 40, 2115–2129, 1993.
- Copin-Montegut, C.: Alkalinity and carbon budgets in the Mediterranean Sea, *Global Biogeochem. Cy.*, 7, 915–925, 1993.
- Crise, A., Allen, J. I., Baretta, J., Crispi, G., Mosetti, R., and Solidoro, C.: The Mediterranean pelagic ecosystem response to physical forcing, *Prog. Oceanogr.*, 44, 219–243, 1999.
- Dickson, A. G.: Thermodynamics of the dissociation of boric acid in synthetic seawater from 273.15 to 318.15 K, *Deep-Sea Res.*, 37, 755–766, 1990.
- Dickson, A. G. and Millero, F. J.: A comparison of the equilibrium constants for the dissociation of carbonic acid in seawater media, *Deep-Sea Res.*, 34A, 1733–1743, 1987.
- D'Ortenzio, F. and Ribera d'Alcalà, M.: On the trophic regimes of the Mediterranean Sea: a satellite analysis, *Biogeosciences*, 6, 139–148, doi:10.5194/bg-6-139-2009, 2009.
- Eggleston, E. S., Sabine, C. L., and Morel, F. M. M.: Revelle revisited: Buffer factors that quantify the response of ocean chemistry to changes in DIC and alkalinity, *Global Biogeochem. Cy.*, 24, GB1002, doi:10.1029/2008GB003407, 2010.
- Goyet, C. and Poisson, A.: New determination of carbonic acid dissociation constants in seawater as a function of temperature and salinity, *Deep-Sea Res.*, 36, 1635–1654, 1989.
- Hainbucher, D., Rubino, A., Cardin, V., Tanhua, T., Schroeder, K., and Bensi, M.: Hydrographic situation during cruise M84/3 and P414 (spring 2011) in the Mediterranean Sea, *Ocean Sci. Discuss.*, 10, 2399–2432, doi:10.5194/osd-10-2399-2013, 2013.
- Hansson, I.: A new set of acidity constants for carbonic acid and boric acid in sea water, *Deep-Sea Res.*, 20, 4611–478, 1973a.
- Hansson, I.: The determination of dissociation constants of carbonic acid in synthetic sea water in the salinity range of 20–40‰ and temperature range of 5–30 °C, *Acta Chemica Scandinavia*, 27, 931–944, 1973b.
- Hernández-Ayón, J. M., Belli, S. L., and Zirino, A.: pH, alkalinity, and total CO₂ in coastal seawater by potentiometric titration with a difference derivative readout, *Anal. Chim. Acta*, 394, 101–108, 1999.
- Hopkins, T. S.: Recent observations on the intermediate and deep water circulation in the Southern Tyrrhenian Sea, *Oceanol. Acta*, 9, 41–50, 1988.
- Huertas, I. E., Ríos, A. F., García-Lafuente, J., Navarro, G., Makaoui, A., Sánchez-Román, A., Rodríguez-Galvez, S., Orbi, A., Ruíz, J., and Pérez, F.F.: Atlantic forcing of the Mediterranean oligotrophy, *Global Biogeochem. Cy.*, 26, GB2022, doi:10.1029/2011GB004167, 2012.
- Ignatiades, L., Gotsis-Skretas, O., Pagou, K., and Krasakopoulou, E.: Diversification of phytoplankton community structure and related parameters along a large-scale longitudinal east-west transect of the Mediterranean Sea, *J. Plankton. Res.*, 31, 411–428, 2009.
- Key, R. M., Kozyr, A., Sabine, C. L., Lee, K., Wanninkhof, R., Bullister, J. L., Feely, R. A., Millero, F. J., Mordy, C., and Peng, T.-H.: A global ocean carbon climatology: Results from Global Data Analysis Project (GLODAP), *Global Biogeochem. Cy.*, 18, GB4031, doi:10.1029/2004GB002247, 2004.
- Key, R. M., Tanhua, T., Olsen, A., Hoppema, M., Jutterström, S., Schirnack, C., van Heuven, S., Kozyr, A., Lin, X., Velo, A., Wallace, D. W. R., and Mintrop, L.: The CARINA data synthesis project: introduction and overview, *Earth Syst. Sci. Data*, 2, 105–121, doi:10.5194/essd-2-105-2010, 2010.
- Khoo, K. H., Ramette, R. W., Culbertson, C. H., and Bates, R. G.: Determination of hydrogen ion concentrations in seawater from

- 5 to 40 °C: standard potentials at salinities from 20 to 45 ‰, *Anal. Chemist.*, 49, 29–34, 1977.
- Kleypas, J. A., McManus, J. W., and Meñez, L. A. B.: Environmental limits to coral reef development: where do we draw the line?, *Am. Zool.*, 39, 146–159, 1999.
- Krasakopoulou, E., Souvermezoglou, E., and Goyet, C.: Anthropogenic CO₂ fluxes in the Otranto strait (E. Mediterranean) in February 1995, *Deep-Sea Res. I*, 58, 1103–1114, 2011.
- Krom, M. D., Woodward, E. M. S., Herut, B., Kress, N., Carbo, P., Mantoura, R. F. C., Spyres, G., Thingstad, T. F., Wassmann, P., Wexels-Riser, C., Kitidis, V., Law, C. S., and Zodiatis, G.: Nutrient cycling in the south east Levantine basin of the eastern Mediterranean: results from a phosphorus starved system, *Deep Sea Res. II*, 52, 2879–2896, 2005.
- Lazzari, P., Solidoro, C., Ibello, V., Salon, S., Teruzzi, A., Béranger, K., Colella, S., and Crise, A.: Seasonal and inter-annual variability of plankton chlorophyll and primary production in the Mediterranean Sea: a modelling approach, *Biogeosciences*, 9, 217–233, doi:10.5194/bg-9-217-2012, 2012.
- Lee, K., Millero, F. J., and Wanninkhof, R.: The carbon dioxide system in the Atlantic Ocean, *J. Geophys. Res.*, 102, 15693–15707, doi:10.1029/97JC00067, 1997.
- Lee, K., Kim, T.-W., Byrne, R. H., Millero, F. J., Feely, R. A., and Liu, M.-M.: The universal ratio of boron to chlorinity for the North Pacific and North Atlantic Oceans, *Geochim. Cosmochim. Acta*, 74, 1801–1811, 2010.
- Lee, K., Sabine, C. L., Tanhua, T., Kim, T. W., Feely, R. A., and Kim, H. C.: Roles of marginal seas in absorbing and storing fossil fuel CO₂, *Energy Environ. Sci.*, 4, 1133–1146, doi:10.1039/C0EE00663G, 2011.
- Luchetta, A., Cantoni, C., and Catalano, G.: New observations of CO₂ induced acidification in the Northern Adriatic Sea over the last quarter century, *Chem. Ecol.*, 26, 1–17, doi:10.1080/02757541003627688, 2010.
- Ludwig, W., Bouwman, A. F., Dumont, E., and Lespina, F.: Water and nutrient fluxes from major Mediterranean and Black Sea rivers: Past and future trends and their implications for the basin-scale budgets, *Global Biogeochem. Cy.*, 24, GB0A13, doi:10.1029/2009GB003594, 2010.
- Lueker, T. J., Dickson, A. G., and Keeling, C. D.: Ocean pCO₂ calculated from dissolved inorganic carbon, alkalinity, and equations for K₁ and K₂: validation based on laboratory measurements of CO₂ in gas and seawater at equilibrium, *Mar. Chem.*, 70, 105–119, 2000.
- McCartney, M. S. and Mauritzen, C.: On the origin of the warm inflow to the Nordic Seas, *Prog. Oceanogr.*, 51, 125–214, 2001.
- Mehrbach, C., Culbertson, C. H., Hawley, J. E., and Pytkowicz, R. M.: Measurements of the apparent dissociation constants of carbonic acid in seawater at atmospheric pressure, *Limnol. Oceanogr.*, 18, 897–907, 1973.
- Millero, F. J.: The marine inorganic carbon cycle, *Chem. Rev.*, 107, 308–341, doi:10.1021/cr0503557, 2007.
- Millero, F. J.: Carbonate constants for estuarine waters, *Mar. Freshw. Res.*, 61, 139–142, 2010.
- Millero, F., Morse, J., and Chen, C.-T.: The carbonate system in the western Mediterranean Sea, *Deep-sea Res.*, 26, 1395–1404, 1979.
- Millero, F. J., Pierrot, D., Lee, K., Wanninkhof, R., Feely, R. Sabine, C. L., Key, R. M., and Takahashi, T.: Dissociation constants for carbonic acid determined from field measurements, *Deep-Sea Res. I*, 49, 1705–1723, 2002.
- Millero, F. J., Graham, T. B., Huang, F., Bustos-Serrano, H., and Pierrot, D.: Dissociation constants of carbonic acid in seawater as a function of salinity and temperature, *Mar. Chem.*, 100, 80–94, 2006.
- Millot, C. and Taupier-Letage, I.: Circulation in the Mediterranean Sea, in: *The Mediterranean Sea, the Handbook of Environmental Chemistry*, Springer, Berlin/Heidelberg, 29–66, 2005.
- Mojica-Prieto, F. J. and Millero, F. J.: The values of pK₁ + pK₂ for the dissociation of carbonic acid in seawater, *Geochim. Cosmochim. Acta*, 66, 2529–2540, 2002.
- Moutin, T. and Raimbault, P.: Primary production, carbon export and nutrients availability in western and eastern Mediterranean Sea in early summer 1996 (MINOS cruise), *J. Marine. Syst.*, 33, 273–288, 2002.
- Park, P. K.: Oceanic CO₂ system: an evaluation of ten methods of investigation, *Limnol. Oceanogr.*, 2, 179–186, 1969.
- Peng, T. H., Takahashi, T., Broecker, W. S., and Olafsson, J.: Seasonal variability of carbon dioxide, nutrients and oxygen in the northern North Atlantic surface water: Observations and model, *Tellus*, 39B, 439–458, 1987.
- Pérez, F. F. and Fraga, F.: A precise and rapid analytical procedure for alkalinity determination, *Mar. Chem.*, 21, 169–182, 1987.
- Pérez, F. F., Ríos, A. F., Rellán, T., and Álvarez, M.: Improvements in a fast potentiometric seawater alkalinity determination, *Cienc. Mar.*, 26, 463–478, 2000.
- Pujo-Pay, M., Conan, P., Oriol, L., Cornet-Barthaux, V., Falco, C., Ghiglione, J.-F., Goyet, C., Moutin, T., and Prieur, L.: Integrated survey of elemental stoichiometry (C, N, P) from the western to eastern Mediterranean Sea, *Biogeosciences*, 8, 883–899, doi:10.5194/bg-8-883-2011, 2011.
- Rahav, E., Herut, B., Levi, A., Mulholland, M. R., and Berman-Frank, I.: Springtime contribution of dinitrogen fixation to primary production across the Mediterranean Sea, *Ocean Sci.*, 9, 489–498, doi:10.5194/os-9-489-2013, 2013.
- Ribera d'Alcalà, M., Civitaresse, G., Conversano, F., and Lavezza, R.: Nutrient ratios and fluxes hint at overlooked processes in the Mediterranean Sea, *J. Geophys. Res.*, 108, 8106, doi:10.1029/2002JC001650, 2003.
- Ricke, K. L., Orr, J. C., Schneider, K., and Caldeira, K.: Risks to coral reefs from ocean carbonate chemistry changes in recent earth system model projections, *Environ. Res. Lett.*, 8, 034003, doi:10.1088/1748-9326/8/3/034003, 2013.
- Rivaro, P., Messa, R., Massolo, S., and Frache, R.: Distributions of carbonate properties along the water column in the Mediterranean Sea: Spatial and temporal variations, *Mar. Chem.*, 121, 236–245, 2010.
- Robinson, A. R. and Golnaraghi, M.: The Physical and Dynamical Oceanography of the Mediterranean Sea, in: *Ocean Processes in Climate Dynamics: Global and Mediterranean Examples*, edited by: Malanotte-Rizzoli, R. and Robison, A. R., NATO ASI Series Volume 419, 255–306, 1994.
- Robinson, A. R., Leslie, W. G., Theocharis, A., and Lascaratos, A.: *Mediterranean Sea Circulation*, Encyclopedia of Ocean Sciences, Academic Press, 1689–1706, 2001.
- Roether, W., Klein, B., Manca, B. B., Theocharis, A., and Kioroglou, S.: Transient Eastern Mediterranean deep waters in

- response to the massive dense-water output of the Aegean Sea in the 1990s, *Progr. Ocean.*, 74, 540–571, 2007.
- Roether, W., Manca, B. B., Klein, B., Bregant, D., Georgopoulos, D., Beitzel, V., Kovacevich, V., and Lucchetta, A.: Recent changes in Eastern Mediterranean deep waters, *Science*, 271, 333–335, 1996.
- Roy, R. N., Roy, L. N., Vogel, K. M., Porter-Moore, C., Pearson, T., Good, C. E., Millero, F. J., and Campbell, D. M.: The dissociation constants of carbonic acid in seawater at salinities 5 to 45 and temperatures 0 to 45 °C, *Mar. Chem.*, 44, 249–267, 1993.
- Rubino, A. and Hainbucher, D.: A large abrupt change in the abyssal water masses of the eastern Mediterranean, *Geophys. Res. Lett.*, 34, L23607, doi:10.1029/2007GL031737, 2007.
- Schneider, A., Wallace, D. W. R., and Kortzinger, A.: Alkalinity of the Mediterranean Sea, *Geophys. Res. Lett.*, 34, L15608, doi:10.1029/2006GL028842, 2007.
- Schneider, A., Tanhua, T., Körtzinger, A., and Wallace, D. W. R.: High anthropogenic carbon content in the eastern Mediterranean, *J. Geophys. Res.*, 115, C12050, doi:10.1029/2010JC006171, 2010.
- Schroeder, K., Gasparini, G. P., Borghini, M., and Delfanti, R.: Biogeochemical tracers and fluxes in the Western Mediterranean Sea, spring 2005, *J. Mar. Systems*, 80, 8–24, 2010.
- Siokou-Frangou, I., Christaki, U., Mazzocchi, M. G., Montresor, M., Ribera d'Alcalá, M., Vaqué, D., and Zingone, A.: Plankton in the open Mediterranean Sea: a review, *Biogeosciences*, 7, 1543–1586, doi:10.5194/bg-7-1543-2010, 2010.
- Stöven, T.: Ventilation processes of the Mediterranean Sea based on CFC-12 and SF₆ measurements, Diploma, Leibniz-Institut für Meereswissenschaften der Mathematisch-naturwissenschaftlichen Fakultät, Christian-Albrecht-Universität zu Kiel, Kiel, 2011.
- Stöven, T. and Tanhua, T.: Ventilation of the Mediterranean Sea constrained by multiple transient tracer measurements, *Ocean Sci. Discuss.*, 10, 1647–1705, doi:10.5194/osd-10-1647-2013, 2013.
- Takahashi, T., Williams, R. T., and Bos, D. L.: Carbonate chemistry, in: *GEOSECS Pacific Expedition*, edited by: Broecker, W. S., Spencer, D. W., and Craig, H., Volume 3, Hydrographic Data 1973–1974, National Science Foundation, Washington, D.C., 77–83, 1982.
- Tanhua, T., van Heuven, S., Key, R. M., Velo, A., Olsen, A., and Schirnick, C.: Quality control procedures and methods of the CARINA database, *Earth Syst. Sci. Data*, 2, 35–49, doi:10.5194/essd-2-35-2010, 2010.
- Tanhua, T., Álvarez, M., and Mintrop, L.: Carbon Dioxide, Hydrographic, and Chemical Data Obtained During the R/V Meteor MT84_3 Mediterranean Sea Cruise (5 April–28 April 2011), available at: http://cdiac.ornl.gov/ftp/oceans/CLIVAR/Met_84_3_Med_Sea/, Carbon Dioxide Information Analysis Center, Oak Ridge National Laboratory, US Department of Energy, Oak Ridge, Tennessee, doi:10.3334/CDIAC/OTG.CLIVAR_06MT20110405, 2012.
- Tanhua, T., Hainbucher, D., Schroeder, K., Cardin, V., Álvarez, M., and Civitarese, G.: The Mediterranean Sea system: a review and an introduction to the special issue, *Ocean Sci.*, 9, 789–803, doi:10.5194/os-9-789-2013, 2013a.
- Tanhua, T., Hainbucher, D., Cardin, V., Álvarez, M., Civitarese, G., McNichol, A. P., and Key, R. M.: Repeat hydrography in the Mediterranean Sea, data from the Meteor cruise 84/3 in 2011, *Earth Syst. Sci. Data*, 5, 289–294, doi:10.5194/essd-5-289-2013, 2013b.
- Touratier, F. and Goyet, C.: Decadal evolution of anthropogenic CO₂ in the north western Mediterranean Sea (at the Dyfamed site) from the mid-1990's to the mid-2000's, *Deep-Sea Res. I*, 56, 1708–1716, 2009.
- Touratier, F., Guglielmi, V., Goyet, C., Prieur, L., Pujo-Pay, M., Conan, P., and Falco, C.: Distributions of the carbonate system properties, anthropogenic CO₂, and acidification during the 2008 BOUM cruise (Mediterranean Sea), *Biogeosciences Discuss.*, 9, 2709–2753, doi:10.5194/bgd-9-2709-2012, 2012.
- Uppström, L. R.: The boron/chlorinity ratio of deep-sea water from the Pacific Ocean, *Deep-Sea Res.*, 21, 161–162, 1974.
- van Heuven, S., Pierrot, D., Rae, J. W. B., Lewis, E., and Wallace, D. W. R.: MATLAB Program Developed for CO₂ System Calculations. ORNL/CDIAC-105b. Carbon Dioxide Information Analysis Center, Oak Ridge National Laboratory, U.S. Department of Energy, Oak Ridge, Tennessee, doi:10.3334/CDIAC/otg.CO2SYS_MATLAB_v1.1, 2011.
- Volpe, G., Santoleri, R., Vellucci, V., Ribera d'Alcalà, M., Marullo, S., and D'Ortenzio, F.: The colour of the Mediterranean Sea: Global versus regional bio-optical algorithms evaluation and implication for satellite chlorophyll estimates, *Remote Sens. Environ.*, 107, 625–638, 2007.

1 **Figure S1. Property – property plots showing the M84/3 data from the Levantine basin**
2 **deeper than 500 dbars.** Each plot is self-explanatory. Red lines correspond to stations 291,
3 294 and 296 east of the East Mediterranean Ridge showing the potential temperature –
4 salinity inversion due to Aegean Sea EMDW (Aeg-EMDW) produced during the EMT. Black
5 line corresponds to station 290 and the cyan line to 298. In these stations the former inversion
6 is eroded and deep waters from the Ionian Sea with a lower Aeg-EMDW signature occupy
7 these layers.

8

9 **Figure S2. Property – property plots showing the M84/3 data from the Ionian Sea**
10 **deeper than 600 dbars.** Each plot is self-explanatory. The following stations are highlighted:
11 302 (red line), 303 (cyan line), 305 (green line) and 314 (black line). Station 302 (red line)
12 present the post-EMT situation. Station 314 (black line) in the northern Ionian Sea showing
13 the deepest layers occupied by a saltier overflow from the Adriatic Sea. Stations 302 and 303
14 (cyan and green lines) in the southern Ionian Sea showing the temperature – salinity hook due
15 to the recent input of the saltier overflow from the Adriatic Sea.

16

17 **Figure S3. Property – property plots showing the M84/3 data from the Tyrrhenian Sea**
18 **between 100 and 900 dbars.** Each plot is self-explanatory. The following stations are
19 highlighted: 316 (red line), 319 (cyan line) and 321 (magenta line). Station 319 (cyan line) in
20 the centre of the Tyrrhenian Sea and station 321 (magenta line) in the Sardinia Channel
21 present an aged (high AOU) Levantine Intermediate Water (LIW) associated with its maxima
22 in salinity. Station 316 (red line), the nearest one to Sicily presents a fresher LIW with high
23 AOU and DIC values.

24

25 **Figure S4. Property – property plots showing the M84/3 data from the Tyrrhenian Sea**
26 **deeper than 500 dbars.** Each plot is self-explanatory. The red dots correspond to data deeper
27 than 900 dbars showing the influence of the overflow of Western Mediterranean Deep Water
28 from the western basin.

29

1 **Figure S5. Property – property plots showing the M84/3 data from the Western basin**
2 **deeper than 500 dbars.** Each plot is self-explanatory. The red dots correspond to data deeper
3 than 1500 dbars showing the influence recently formed Western Mediterranean Deep Water.

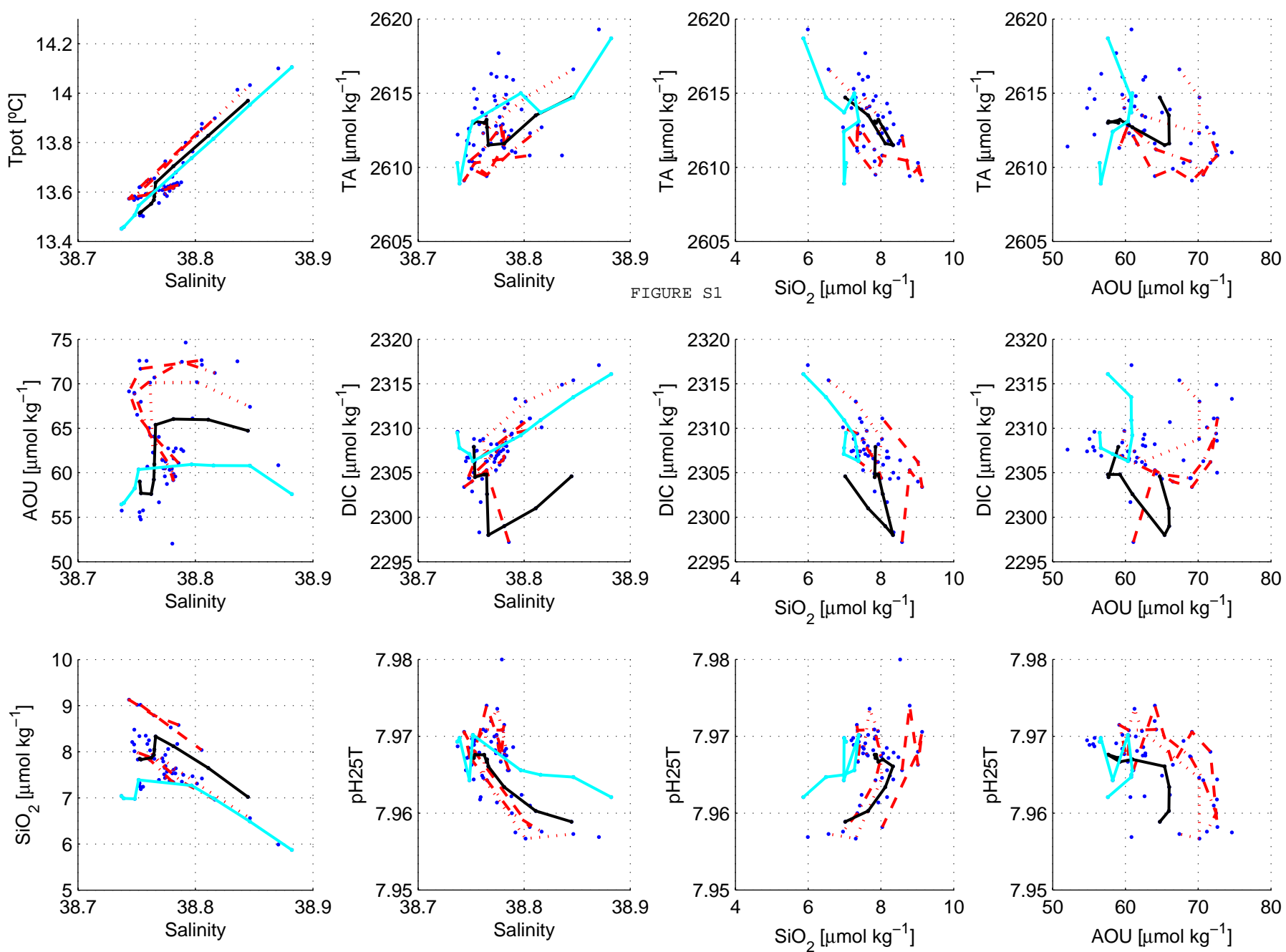
4

5 **Figure S6. Property – property plots showing the M84/3 data in the Strait of Gibraltar**
6 **and Gulf of Cadiz.** Each plot is self-explanatory.

7

8

9



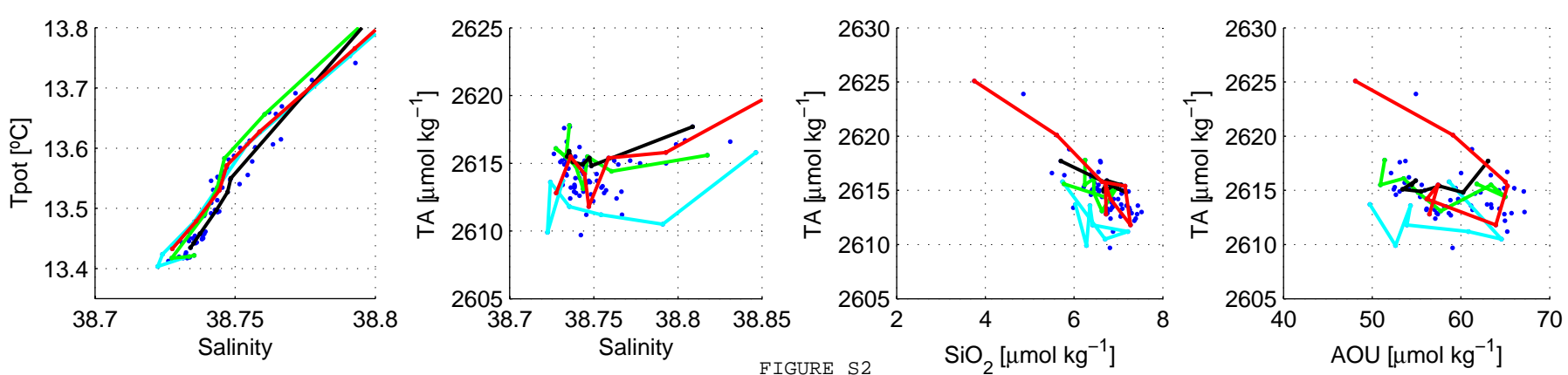
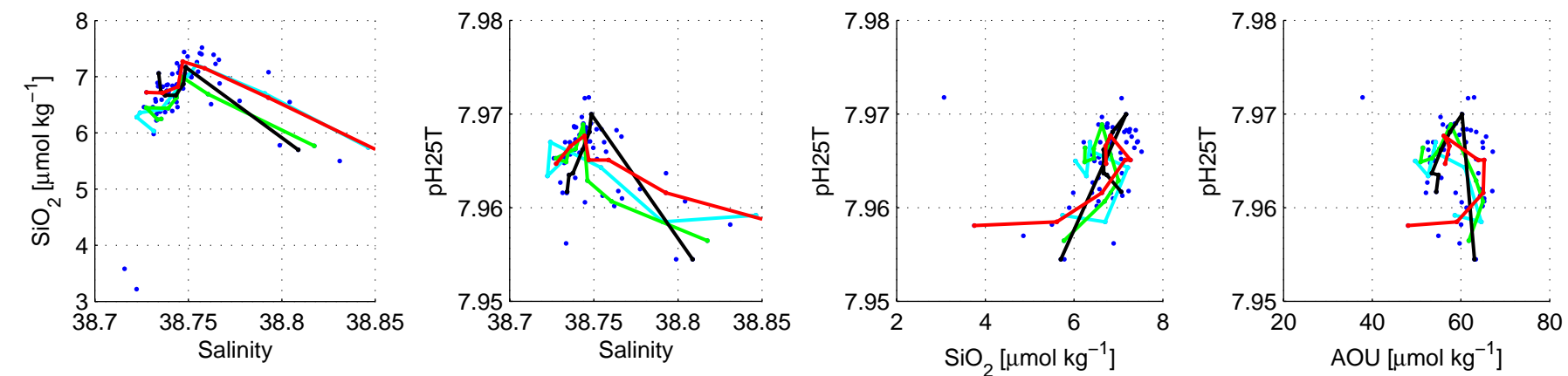
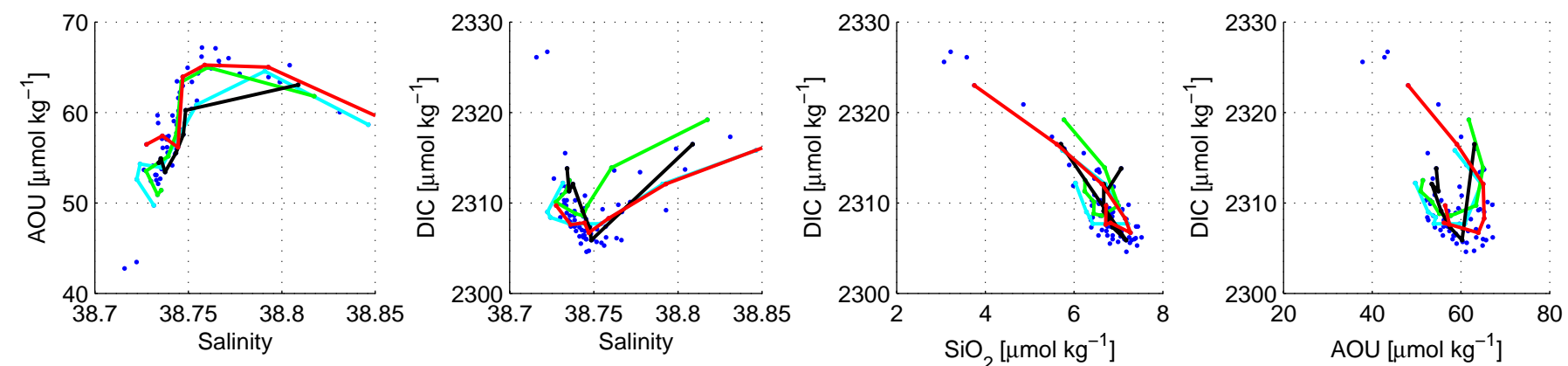


FIGURE S2



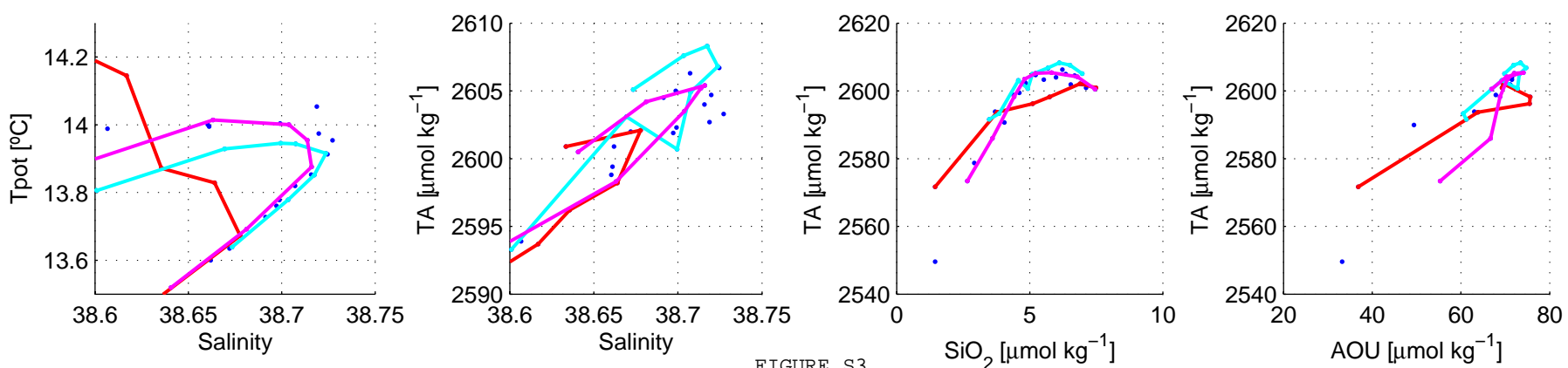
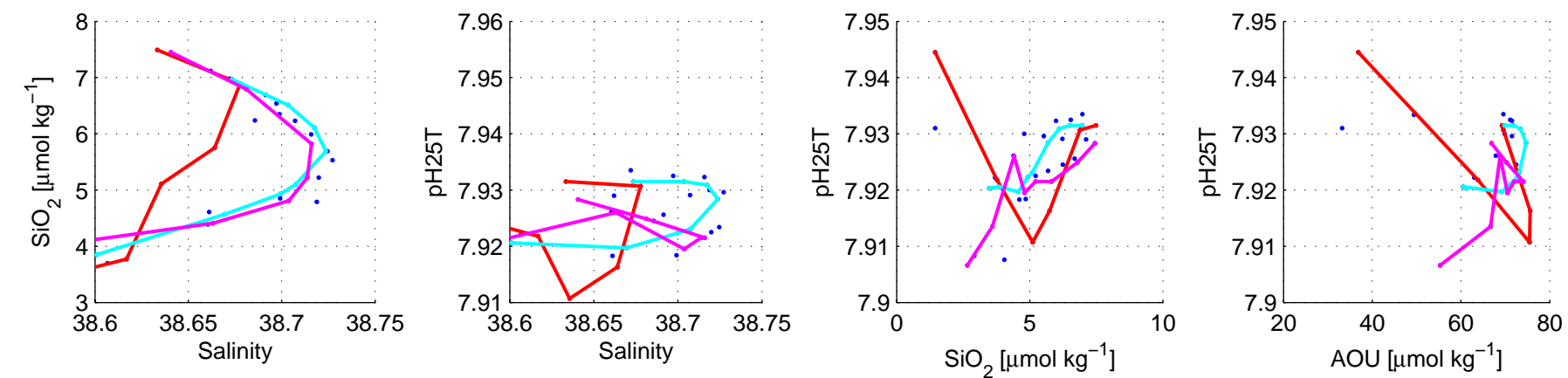
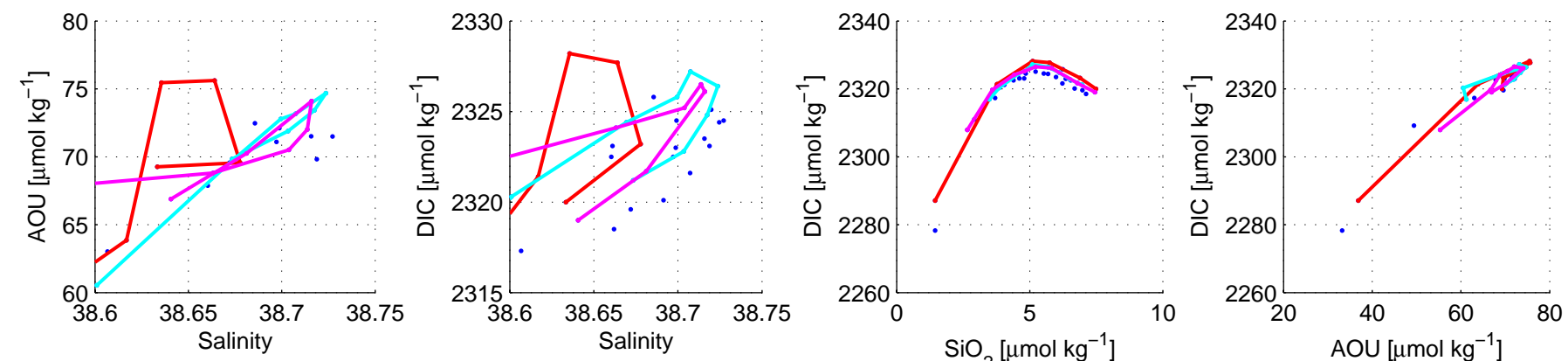


FIGURE S3



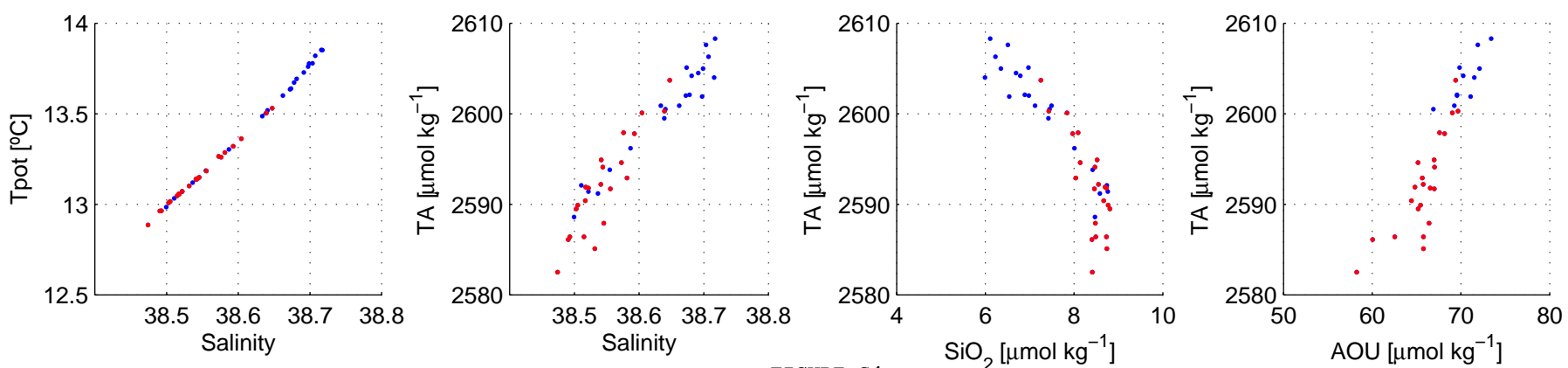
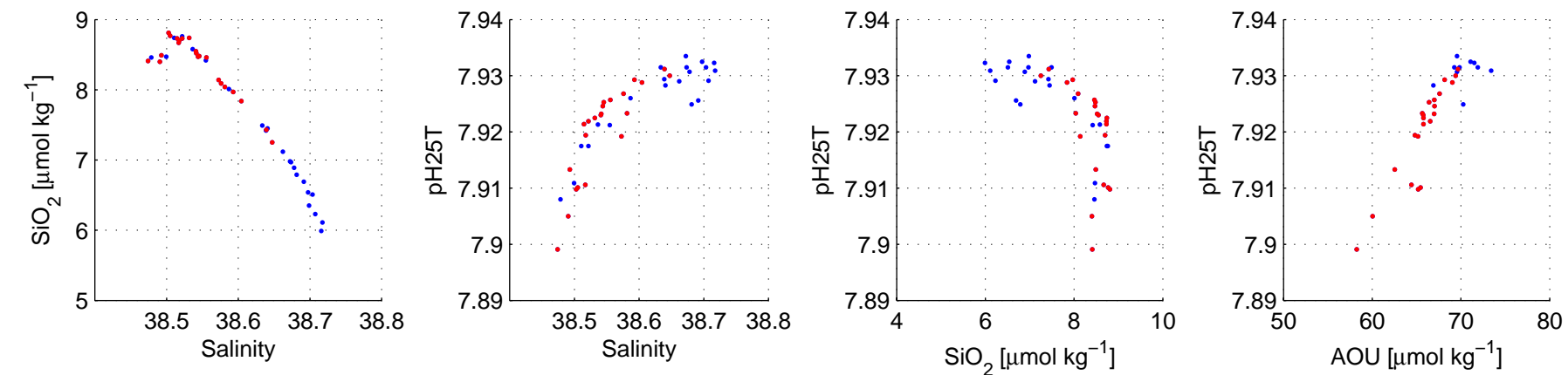
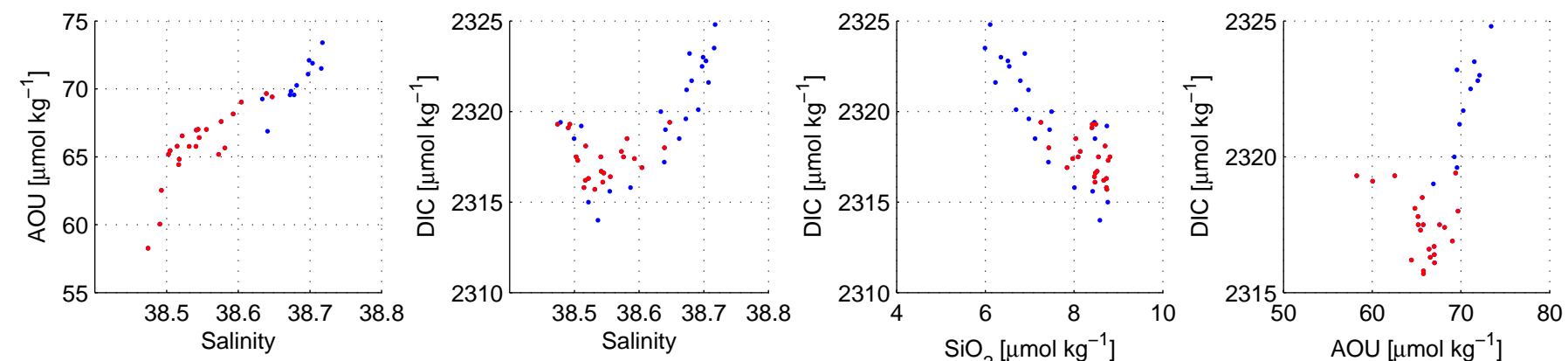
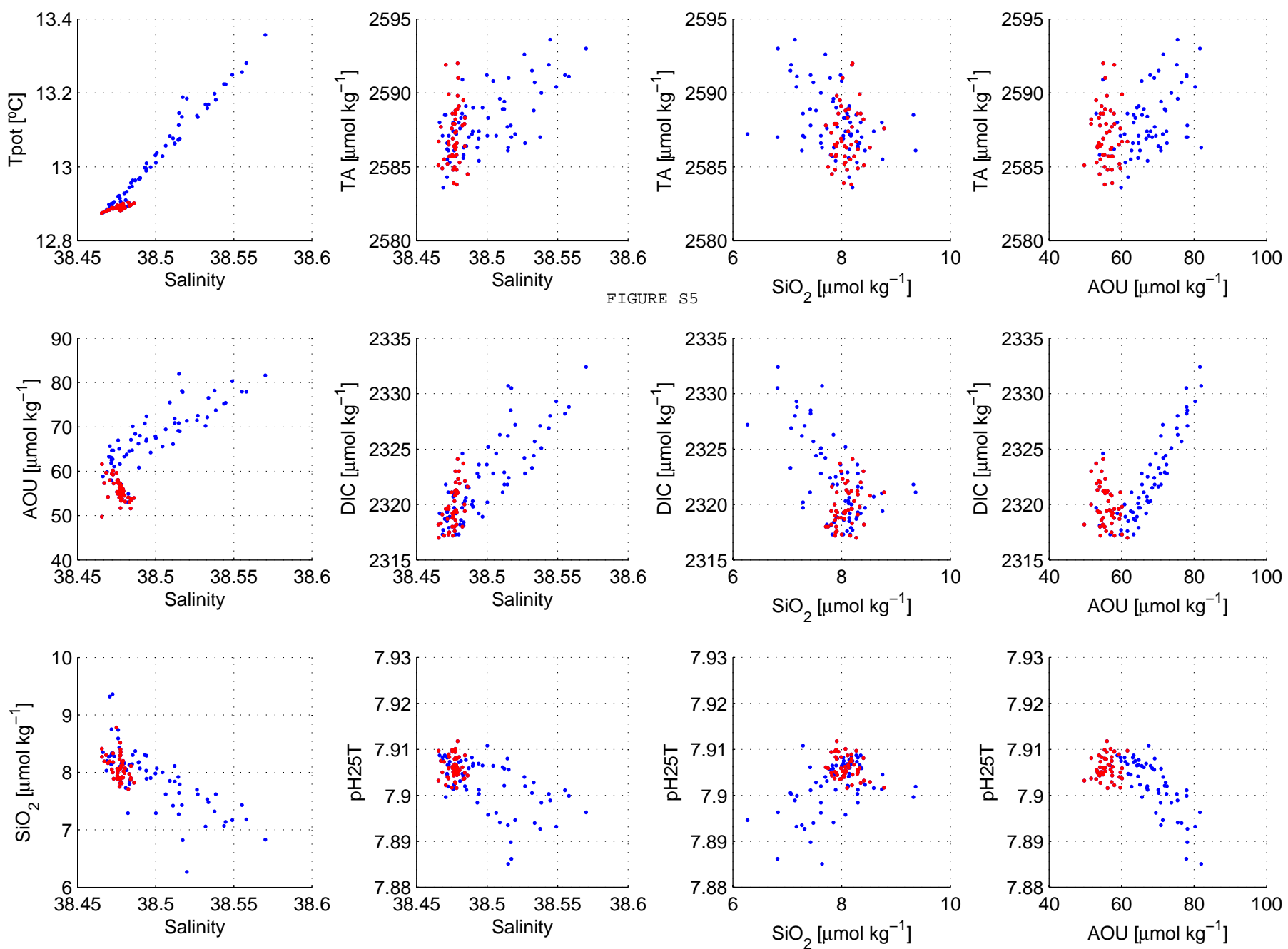


FIGURE S4





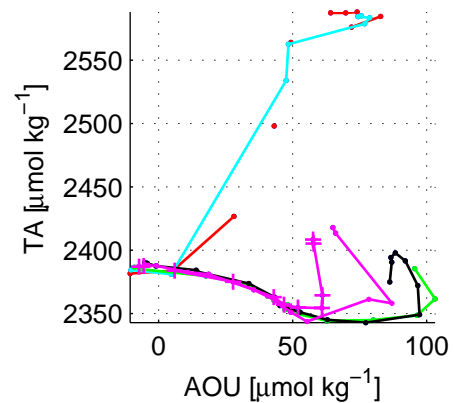
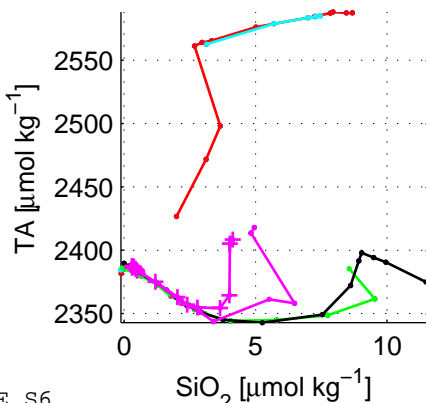
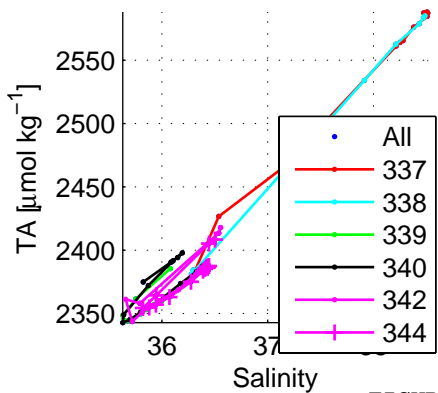
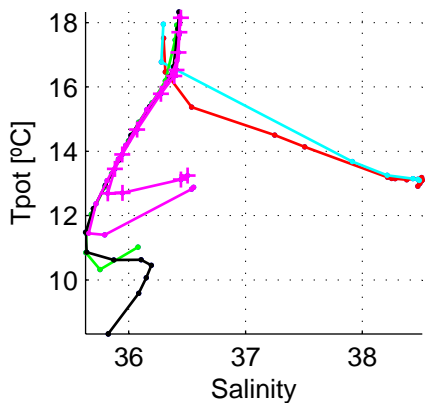


FIGURE S6

